Long-distance contributions in rare $b \to s\bar{\ell}\ell$ decays

Arianna Tinari (University of Zürich)

Based on G. Isidori, Z. Polonsky, AT (2405.17551)

General Meeting of the LHC EFT Working Group
CERN, 2nd-4th December 2024

Universität Zürich[UZH]

Rare $b \to s\bar{\ell}\ell$ decays

- $b \to s\bar{\ell}\ell$ decays are very good candidates in the search for BSM.
- Being suppressed in the SM, they are extremely sensitive to a wide range of NP effects.

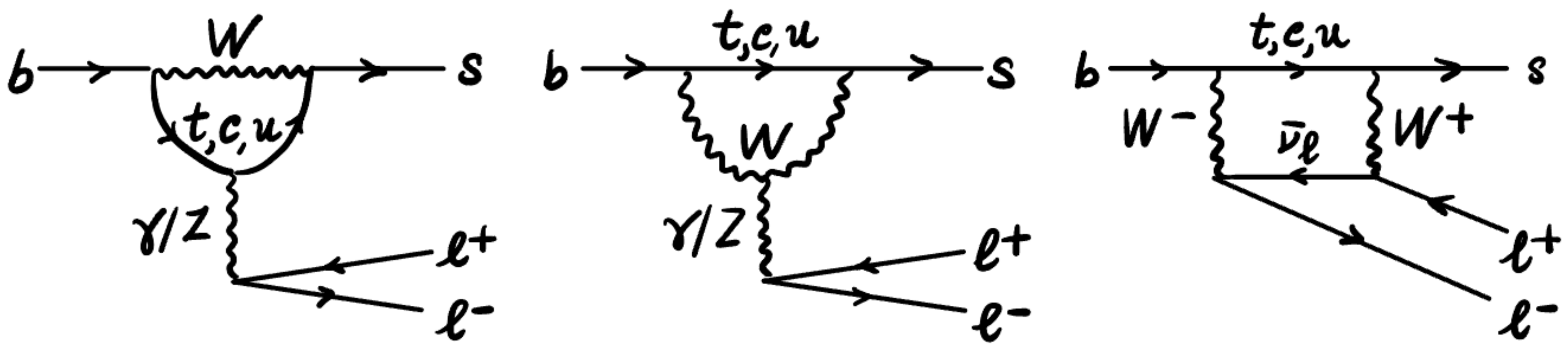

- **Key decay channels** are $B \to K\bar{\ell}\ell, B \to K^*\bar{\ell}\ell, B_s \to \phi\bar{\ell}\ell, B_s \to \bar{\mu}\mu$.
- Observables: **branching ratios**, (optimized) **angular observables** ($P^{(\prime)}_{1,2,3,4,5,6,8}$), **LFU ratios**.
- While LFU ratios are theoretically clean, branching fractions and angular observables are **less clean**, being severely affected by hadronic uncertainties.

Effective Lagrangian

- **Effective description of $b \to s\bar{\ell}\ell$ decays below the EW scale:**

$$\mathscr{L} = \mathscr{L}^{[N_f=5]}_{\mathrm{QCD+QED}} + \frac{4G_F}{\sqrt{2}} V_{tb} V_{ts}^* \sum_{i=1}^{10} C_i \mathcal{O}_i$$

$$\mathcal{O}_1 = \frac{4\pi}{\alpha_e} (\bar{s}_L \gamma_\mu T^a c_L)(\bar{c}_L \gamma^\mu T^a b_L) \qquad \mathcal{O}_2 = \frac{4\pi}{\alpha_e} (\bar{s}_L \gamma_\mu c_L)(\bar{c}_L \gamma^\mu b_L)$$

$$\mathcal{O}_3 = \frac{4\pi}{\alpha_e} (\bar{s}_L \gamma_\mu b_L) \sum_q (\bar{q_L} \gamma^\mu q_L) \qquad \mathcal{O}_4 = \frac{4\pi}{\alpha_e} (\bar{s}^a_L \gamma^\mu T^a b^b_L) \sum_q (\bar{q_L}^b \gamma^\mu T^a q^a_L)$$

$$\mathcal{O}_5 = \frac{4\pi}{\alpha_e} (\bar{s}_L \gamma_\mu \gamma_\nu \gamma_\rho b_L) \sum_q (\bar{q_L} \gamma^\mu \gamma^\nu \gamma^\rho q_R) \qquad \mathcal{O}_6 = \frac{4\pi}{\alpha_e} (\bar{s}^a_L \gamma_\mu \gamma_\nu \gamma_\rho T^a b^b_L) \sum_q (\bar{q_L}^b \gamma^\mu \gamma^\nu \gamma^\rho T^a q^a_R)$$

$$\mathcal{O}_7 = \frac{m_b}{e} (\bar{s}_L \sigma^{\mu\nu} b_R) F_{\mu\nu} \qquad \mathcal{O}_8 = \frac{g_s}{e^2} m_b (\bar{s}_L \sigma^{\mu\nu} T^a b_R) G^a_{\mu\nu}$$

$$\mathcal{O}_9 = (\bar{s}_L \gamma_\mu b_L)(\bar{\ell} \gamma^\mu \ell) \qquad \mathcal{O}_{10} = (\bar{s}_L \gamma_\mu b_L)(\bar{\ell} \gamma^\mu \gamma_5 \ell)$$

- **General features of $b \to s\bar{\ell}\ell$ branching ratios:**
  - q^2 is the invariant mass of the lepton pair.
  - Separate tests in the low- or high-q^2 region.

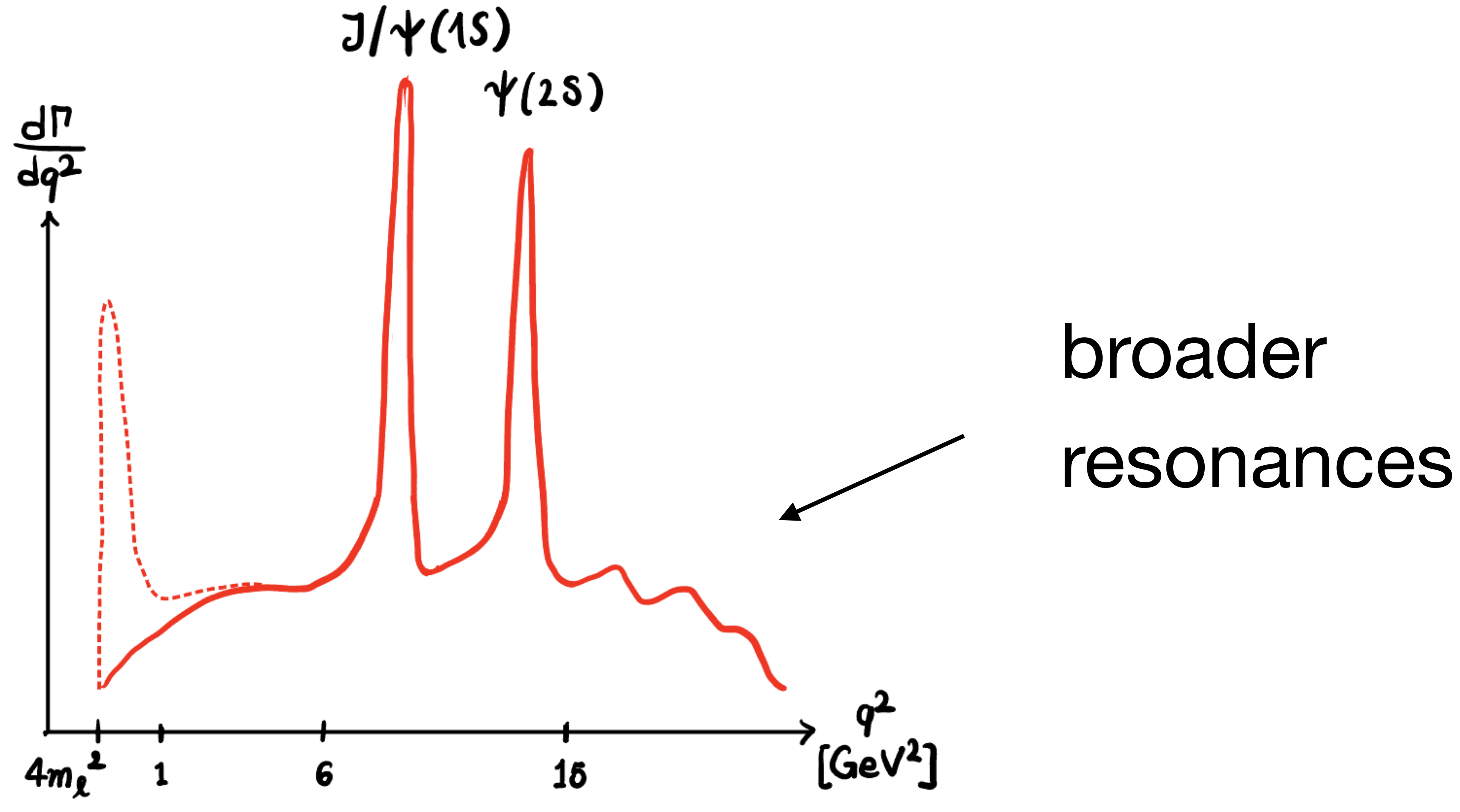

Tension in branching ratios

- Long-standing tension in branching ratios:

$B_s \to \phi\bar{\ell}\ell$

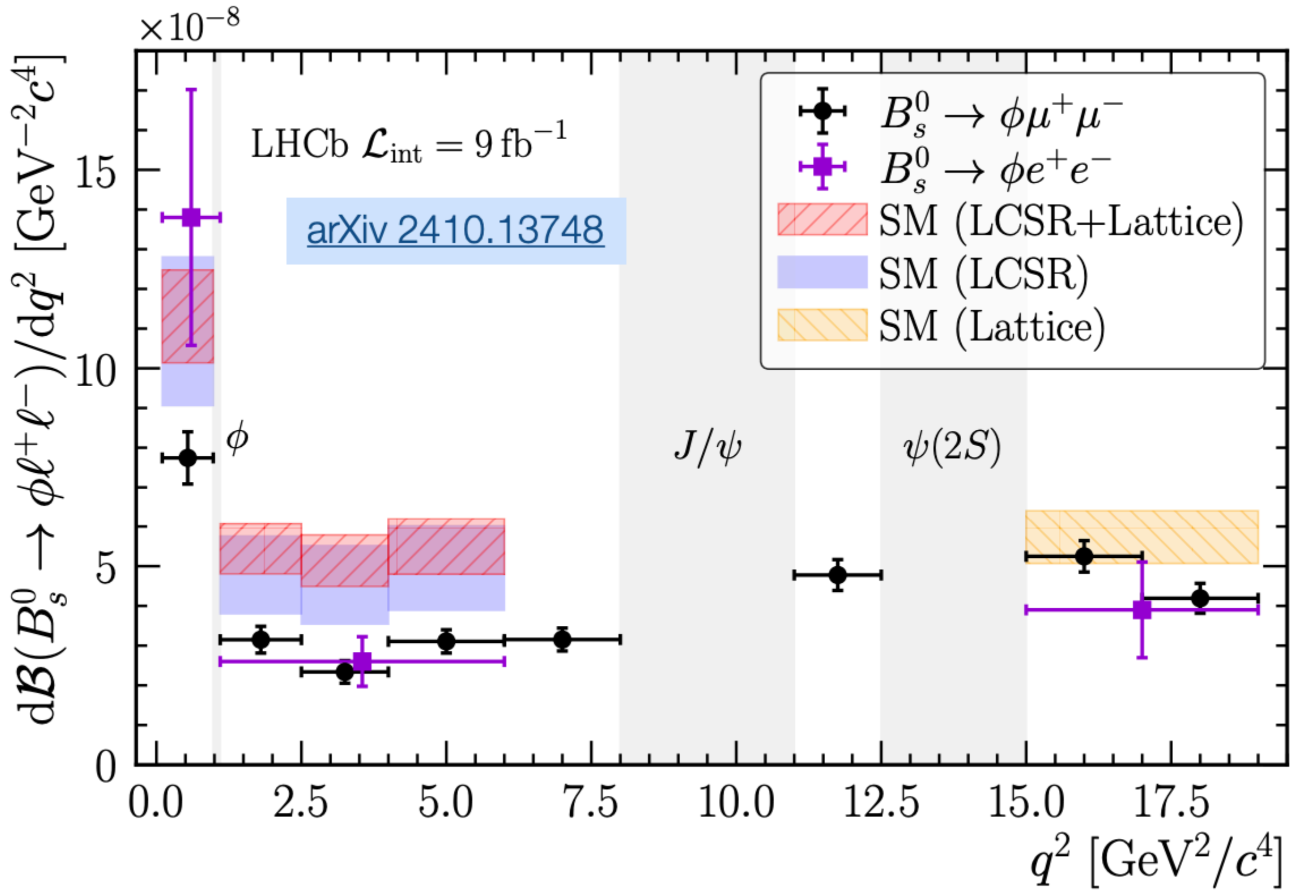

[LHCb, 2410.13748]

$B \to K\bar{\mu}\mu$

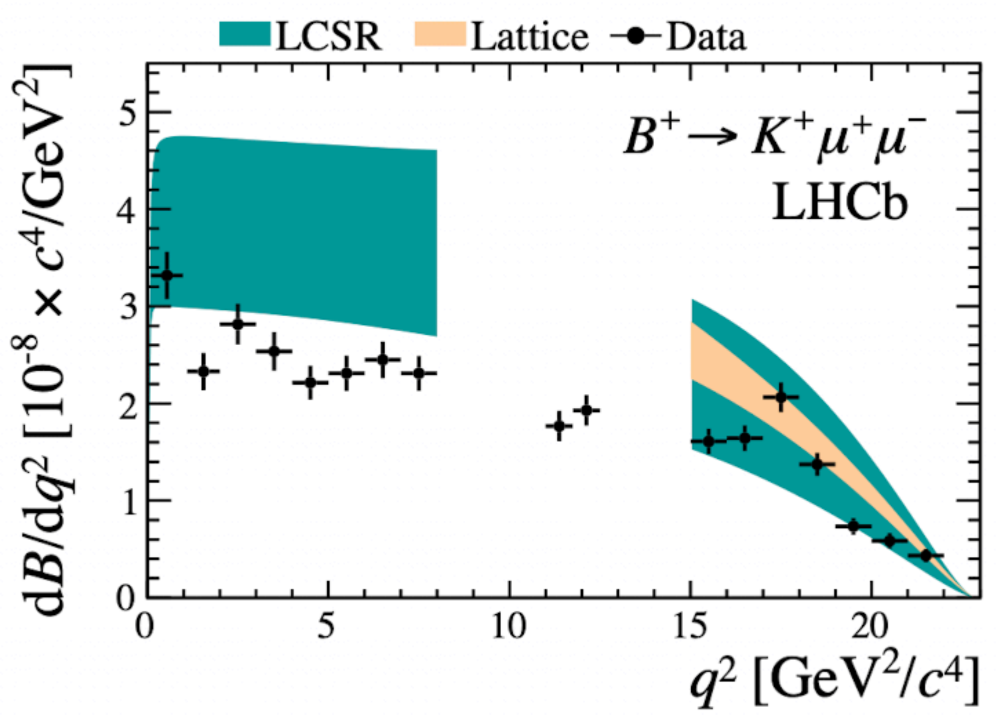

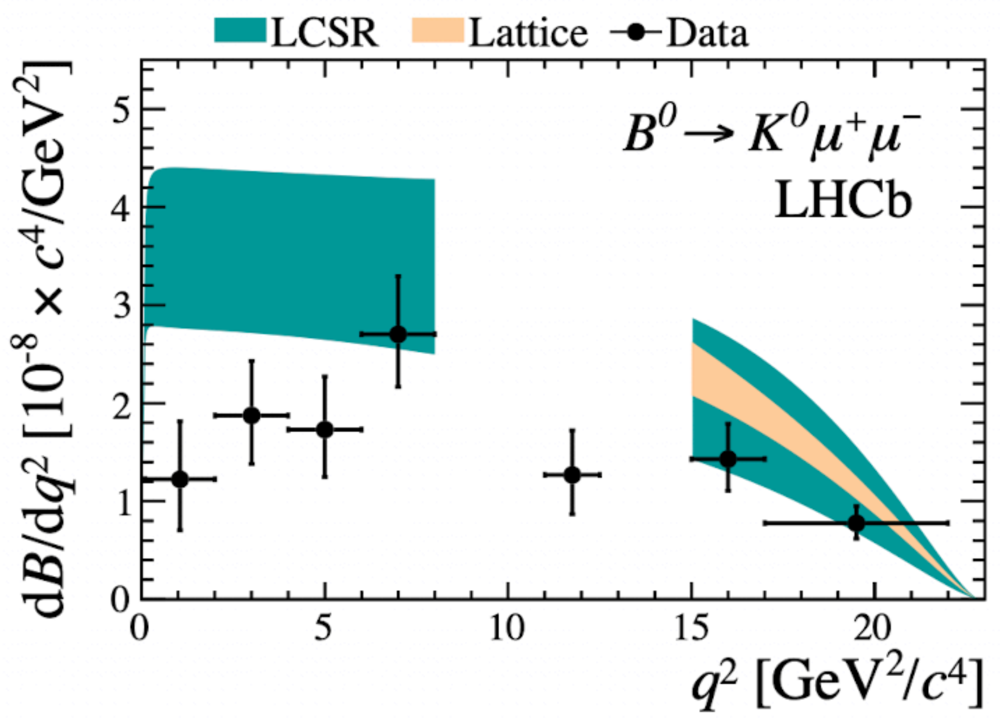

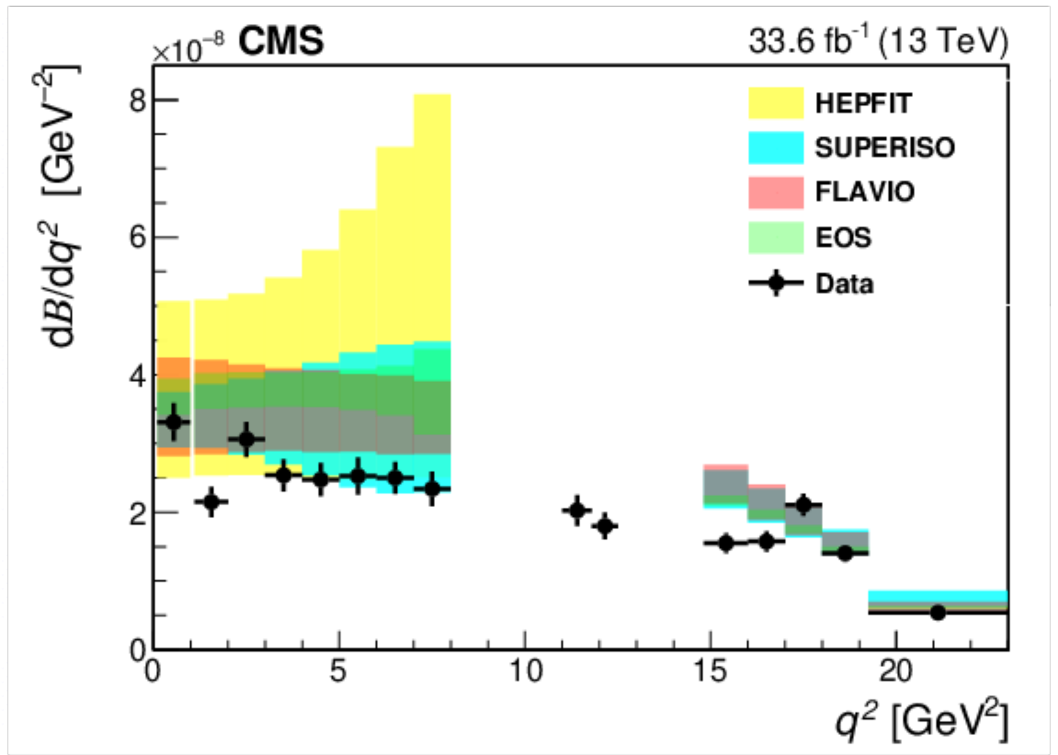

[JHEP 06 (2014) 133]

[CMS: 2401.07090]

$B \to K^*\bar{\mu}\mu$

[LHCb, JHEP 11 (2016) 047]

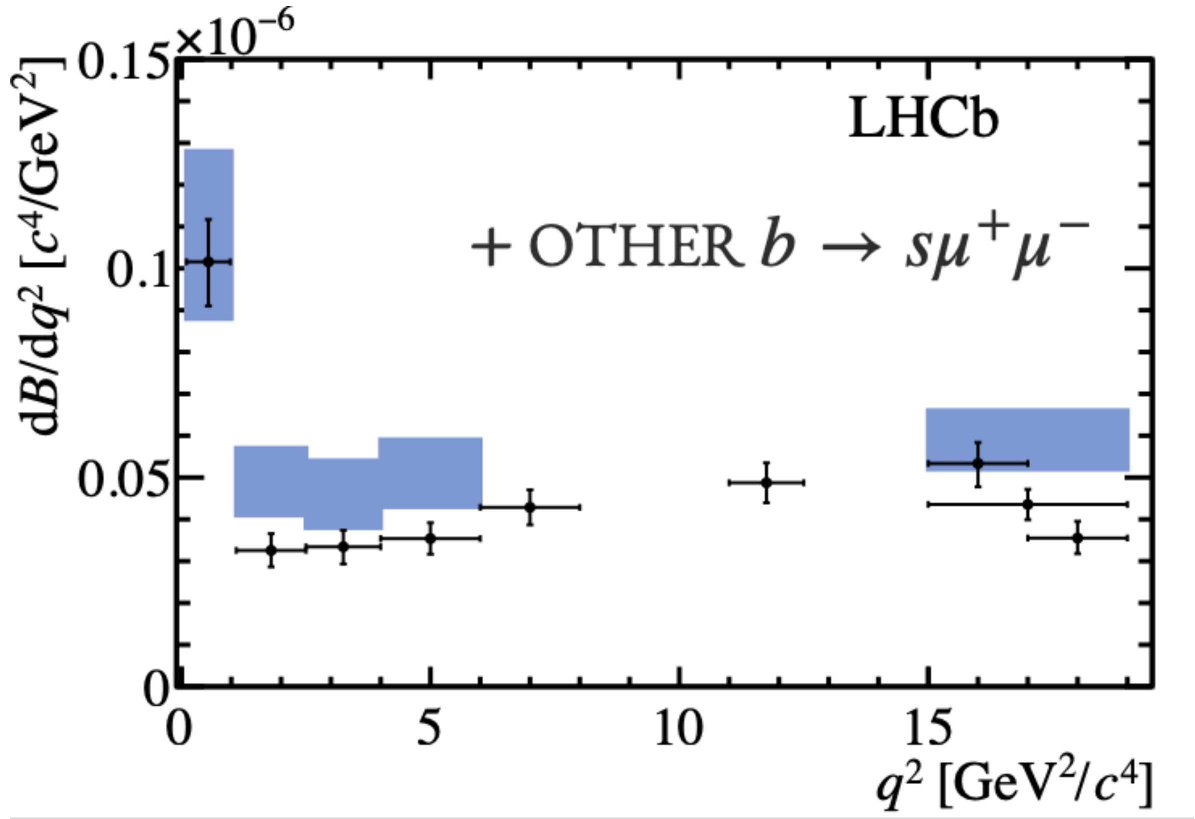

Tension in the inclusive rate

- Tension seen also at the **inclusive level** at high q^2:
  - Compare a semi-inclusive determination based on data from LHCb with the inclusive SM prediction based on:

$$R^{(\ell)}_{\rm incl}(q_0^2) = \frac{\int_{q_0^2}^{m_B^2} dq^2 \frac{d\Gamma(B\to X_s\bar{\ell}\ell)}{dq^2}}{\int_{q_0^2}^{m_B^2} dq^2 \frac{d\Gamma(B\to X_u\bar{\ell}\nu)}{dq^2}} = \frac{|V_{tb}V_{ts}^*|^2}{|V_{ub}|^2}\left[\mathcal{R}_L + \Delta\mathcal{R}_{[q_0^2]}\right]$$

$q_0^2 = 15\ \mathrm{GeV}^2$

from Belle, arXiv:2107.13855

[Z. Ligeti and F. J. Tackmann, 0707.1694]

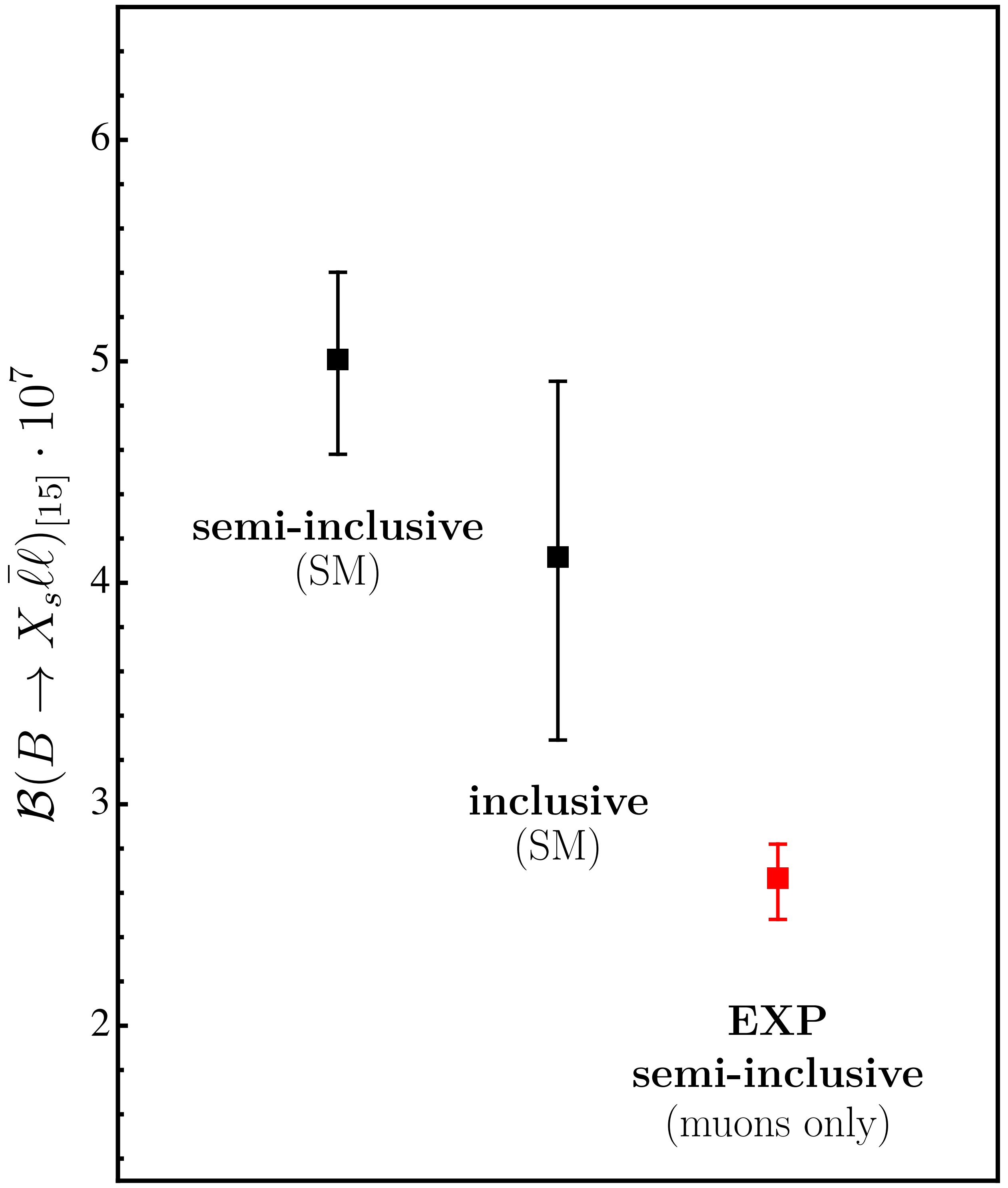

[G.Isidori, Z. Polonsky, AT, 2305.03076]

- The inclusive rate has a **different sensitivity** to non-perturbative effects associated with charm-rescattering and is insensitive to local form factor uncertainties.

Tension in angular observables

- Long-standing tension in angular observables:

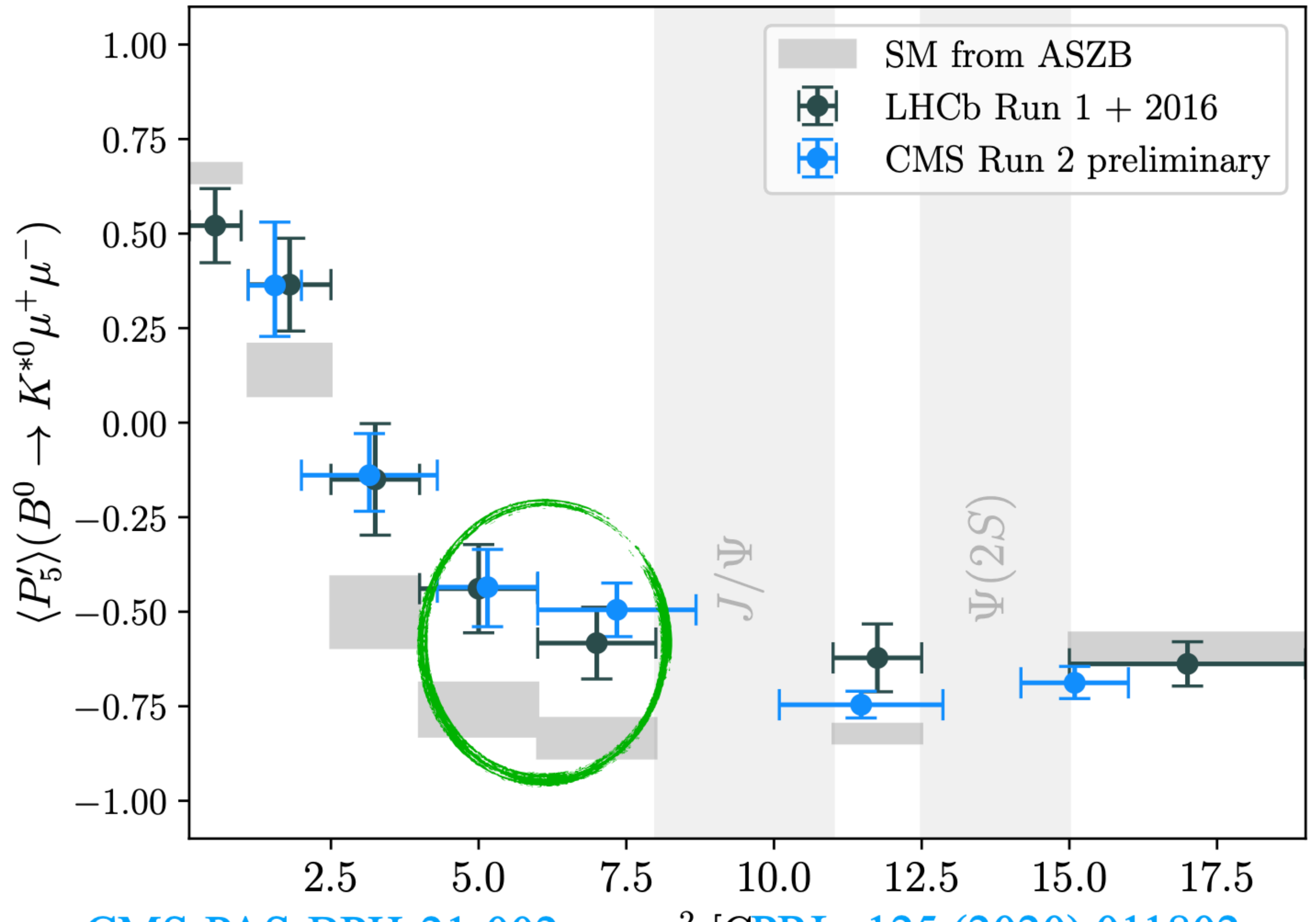

CMS-PAS-BPH-21-002 PRL. 125 (2020) 011802

[Plot by M. Andersson]

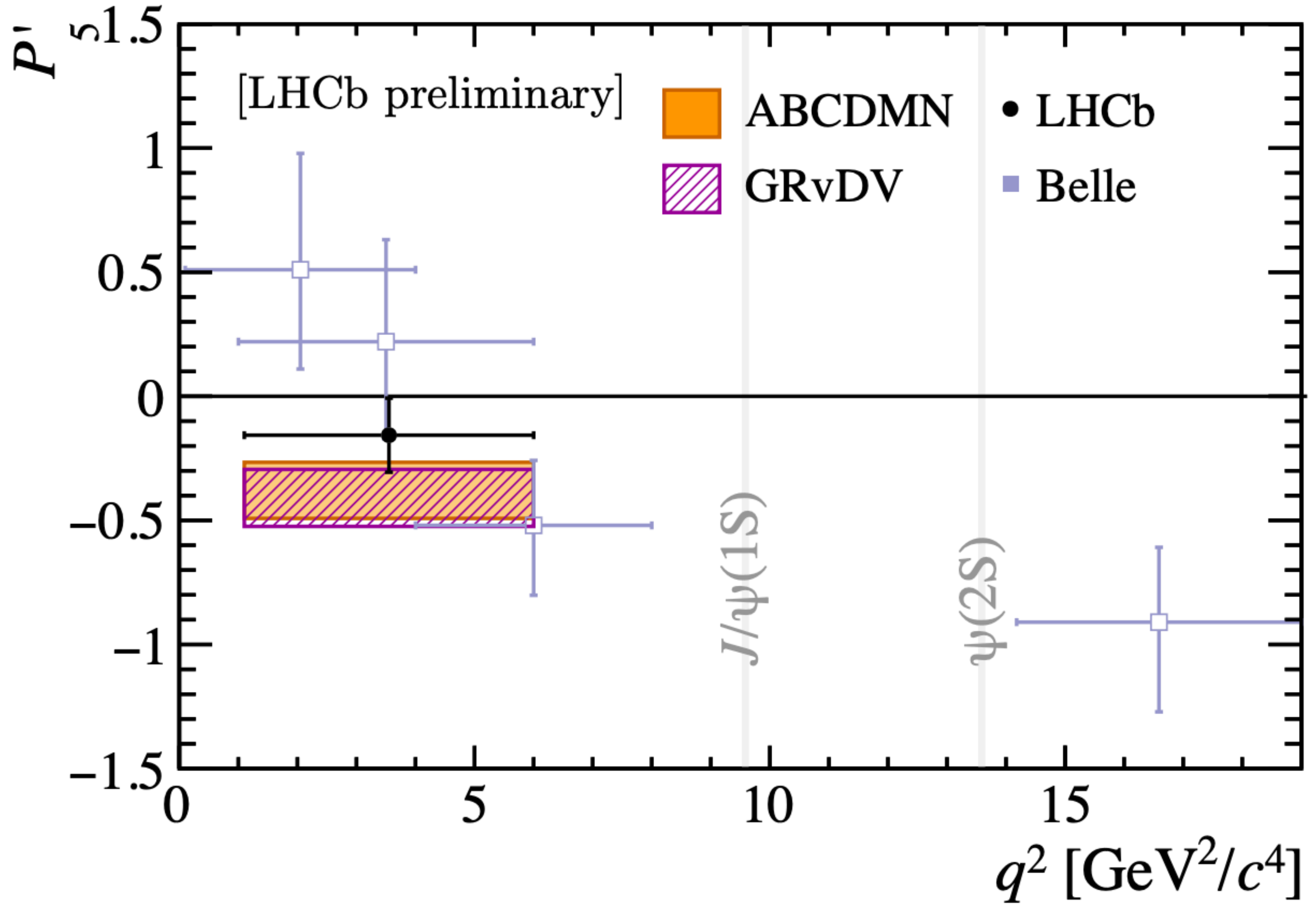

[LHCb-PAPER-2024-022, angular analysis of $B \to K^*\bar{e}e$]

- Recent angular analysis by LHCb on $B \to K^*\bar{\mu}\mu$

[*JHEP* 09 (2024) 026]

see talk by Zahra Gh.Moghaddam

Exclusive modes

* Matrix element for exclusive modes:

$$\mathscr{A}(B \to M\ell^+\ell^-) = \frac{G_F \alpha V_{ts}^* V_{tb}}{\sqrt{2}\pi}\Big[(C_9\ \ell\gamma^\mu\ell + C_{10}\ \ell\gamma^\mu\gamma_5\ell)\langle M|\bar{s}\gamma_\mu P_L b|\bar{B}\rangle\ - \frac{1}{q^2}\ell\gamma^\mu\ell\ (2im_b C_7\langle M|\bar{s}\sigma_{\mu\nu}q^\nu P_R b|B\rangle + \mathscr{H}_\mu)\Big]$$

Local form factors

Lattice QCD + Light-Cone Sum Rules

Bharucha, Straub, Zwicky, 1503.05534

Gubernari, Reboud, van Dyk, Virto, 2305.06301

Non-local form factors

matrix elements of the four-quark operators

$$\mathscr{M}(B \to H_\lambda \ell\ell)|_{C_{1-6}} = -i\frac{32\pi^2\mathscr{N}}{q^2}\bar{\ell}\gamma^\mu\ell\int d^4x e^{iqx}\langle H_\lambda|T\{j_\mu^{\mathrm{em}}(x), \sum_{i=1,6} C_i\mathscr{O}_i(0)\}|B\rangle$$

only $\mathscr{O}_1, \mathscr{O}_2$ give a significant contribution

$$\mathscr{O}_1 = (\bar{s}_L^\alpha\gamma_\mu c_L^\beta)(\bar{c}_L^\beta\gamma^\mu b_L^\alpha) \qquad \mathscr{O}_2 = (\bar{s}_L\gamma_\mu c_L)(\bar{c}_L\gamma^\mu b_L)$$

Exclusive modes

* The non-local form factors contain the matrix elements of the **four-quark operators** $\mathcal{O}_{1-6}$.

* Note that to all orders in α_s, and to first order in α_{em}, **these matrix elements have the same structure as the matrix elements of $\mathcal{O}_7$ and $\mathcal{O}_9$:**

$$\mathcal{M}(B \to H_\lambda \ell\ell)|_{C_{1-6}} = -i\frac{32\pi^2\mathcal{N}}{q^2}\bar{\ell}\gamma^\mu\ell \int d^4x e^{iqx}\langle H_\lambda | T\{j_\mu^{\text{em}}(x), \sum_{i=1,6} C_i\mathcal{O}_i(0)\} | B\rangle = \left(\Delta_9^\lambda(q^2) + \frac{m_B^2}{q^2}\Delta_7^\lambda\right)\langle H_\lambda\, \ell^+\ell^- | \mathcal{O}_9 | B\rangle$$

* The (regular for $q^2 \to 0$) contributions of the non-local matrix elements of the four-quark operators can be effectively taken into account by a **shift in C_9**:

$$C_9 \to C_9^\lambda(q^2) = C_9^{\text{SM}} + \Delta_9^\lambda(q^2) + C_9^{\text{SD}}$$

LD + NP ?

* There is no doubt that the tension with the data could be well described by a shift in C_9 of $\mathcal{O}(25\%)$ with respect to the SM value BUT **this shift could come from an inaccurate description of the non-local matrix elements.**

Non-local contributions

The correlator in $\int d^4x\ e^{iqx}\langle H_\lambda | T\{j_\mu^{\text{em}}(x), \sum_{i=1,6} C_i\mathcal{O}_i(0)\} | B\rangle$ receives two kinds of contributions:

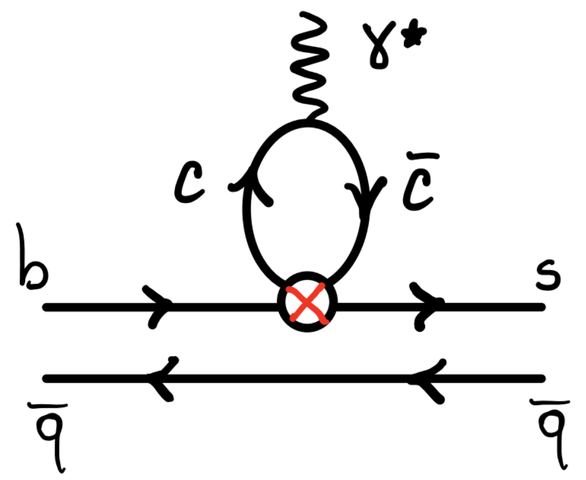

(a)

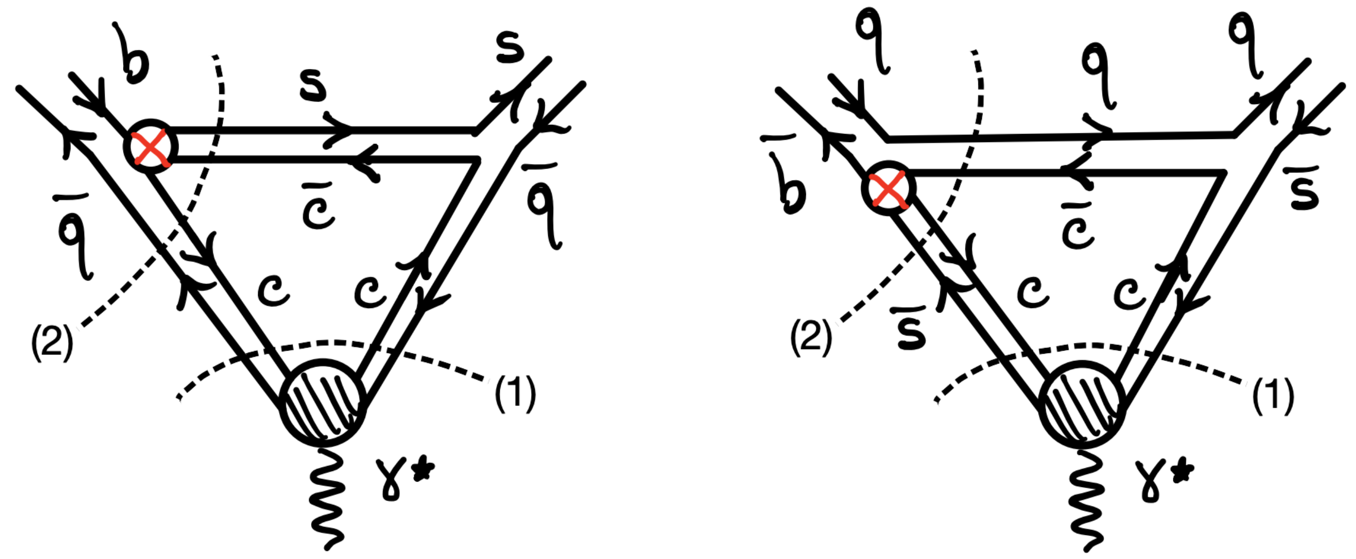

(b)

Pictures from [Ciuchini, Fedele, Franco, Paul, Silvestrini, Valli, 2212.10516]

See Mutke, Hoferichter, Kubis *JHEP* 07 (2024) 276

Second type: **rescattering of a pair of charmed and charmed-strange mesons**.

- Applying dispersive methods is tricky because the analytic structure is quite involved; in particular, an additional singularity in the case of an **anomalous threshold** could move into the q^2 integration domain, requiring a non trivial deformation of the path.
- The effect of these contributions is indistinguishable from a short-distance effect, since they show a **reduced q^2- or λ- dependence.**

Charm rescattering

- These amplitudes are associated with physical thresholds which are not reproduced in any of the non-local theory estimates.
- We look at the simplest decay mode, $B^0 \to K^0 \bar{\ell} \ell$, and the largest contributing two-body intermediate state ($D_s D^*$ and $D_s^* D$).

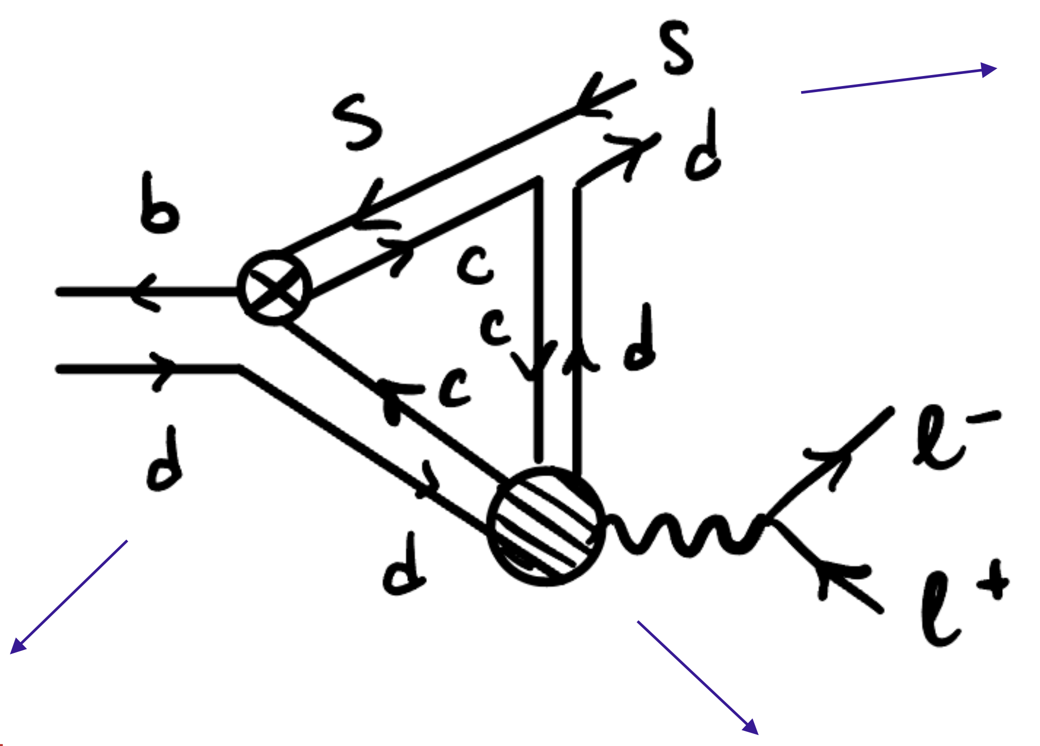

- We obtain an accurate description in the low recoil (or **high** q^2) limit; we extrapolate to the whole kinematical region introducing appropriate form factors.

Charm rescattering

- These amplitudes are associated with physical thresholds which are not reproduced in any of the non-local theory estimates.
- We look at the simplest decay mode, $B^0 \to K^0 \bar{\ell}\ell$, and the largest contributing two-body intermediate state ($D_s D^*$ and $D_s^* D$).

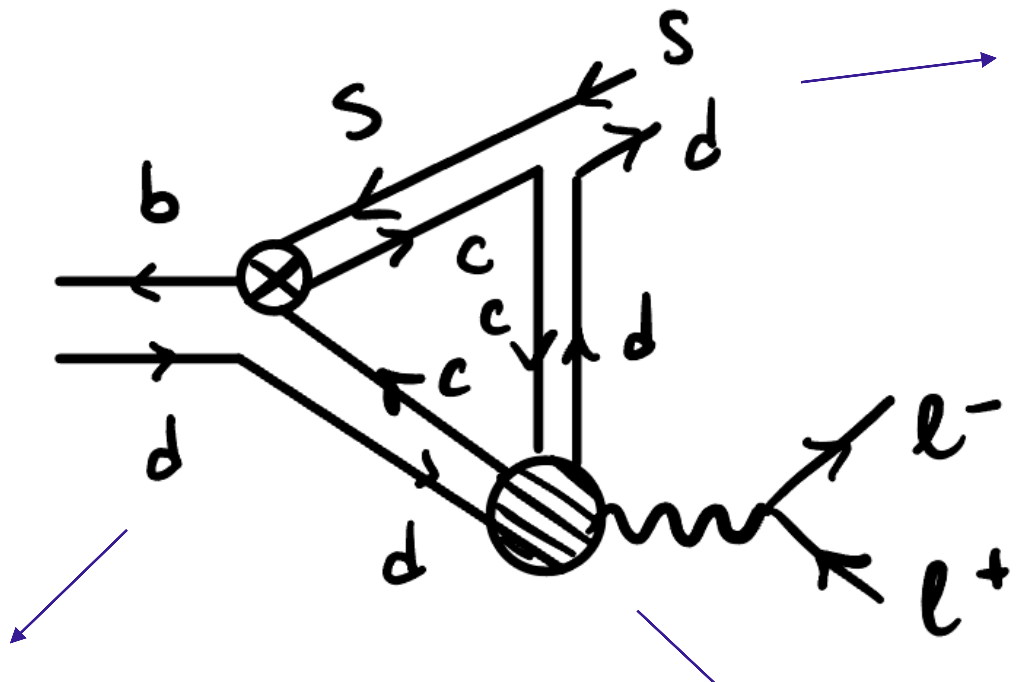

- We obtain an accurate description in the low recoil (or **high** q^2) limit; we extrapolate to the whole kinematical region introducing appropriate form factors.

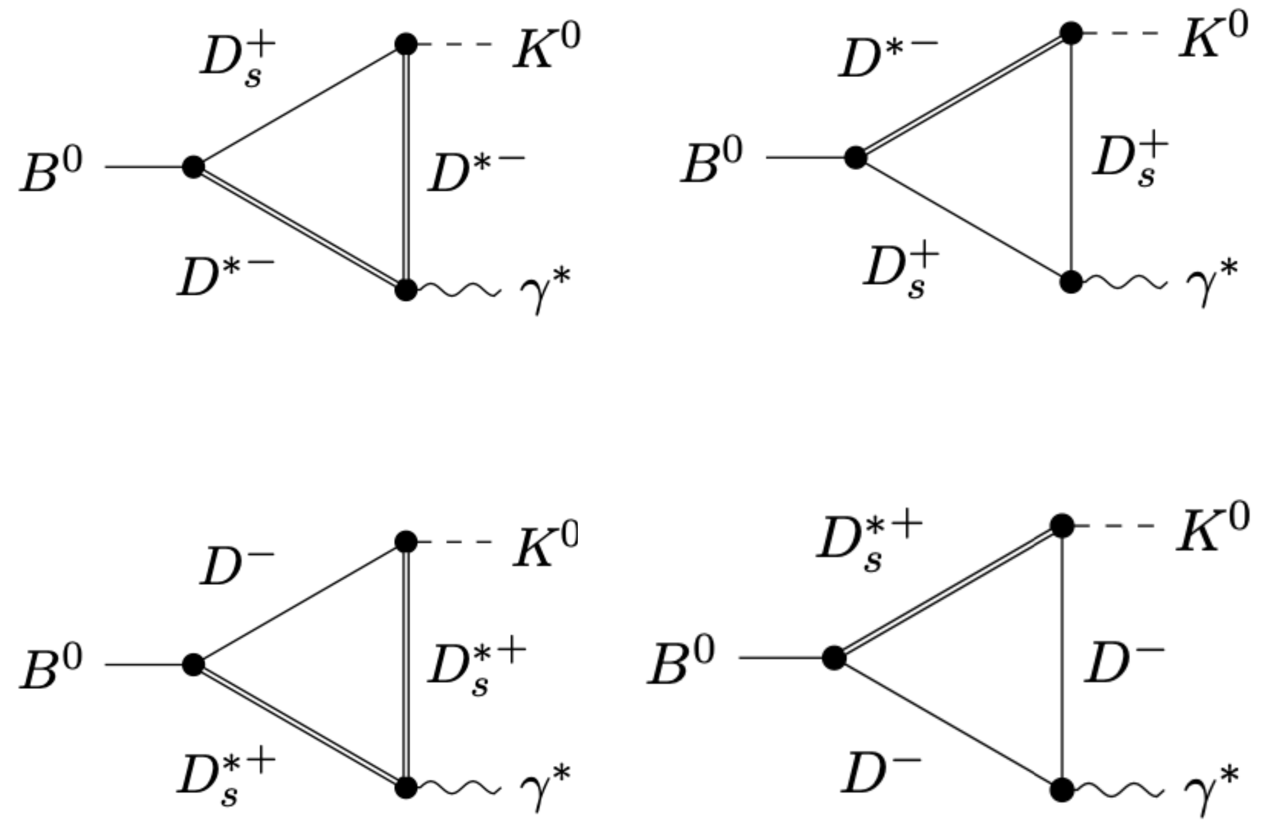

* Goal: estimate topologies where an internal $D^* D_s (D_s^* D)$ pair can go on-shell.
* Simplest effective interactions able to reproduce these discontinuities.
* The model is not meant to analyze rescattering amplitudes associated with different discontinuities, i.e. different intermediate states.

Model

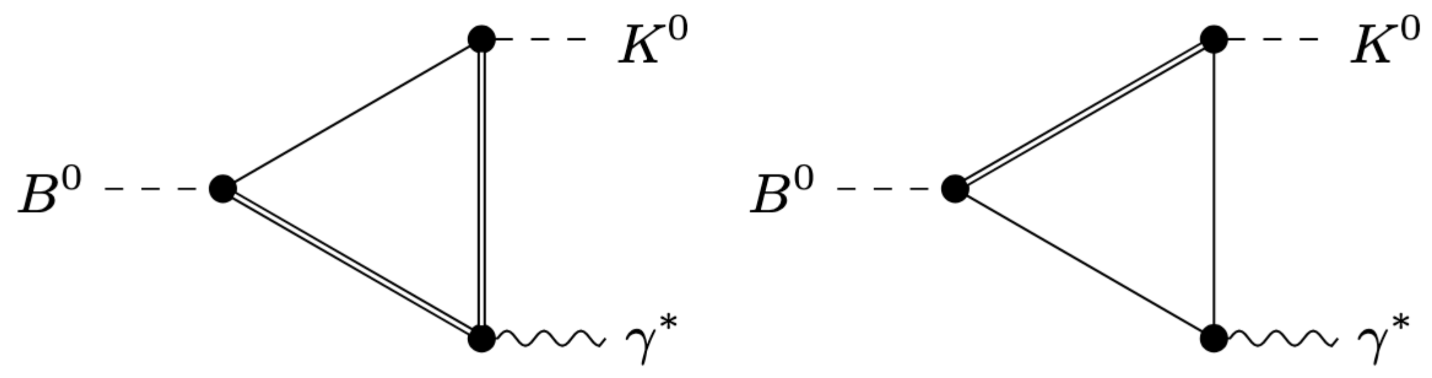

* **Dynamics of $D_{(s)}^{(*)}$ mesons close to their mass shell, determined by:**
    * Lorentz + Gauge invariance under QED
    * $SU(3)$ light-flavor symmetry
    * Heavy-quark spin symmetry

$$
\begin{aligned}
\mathcal{L}_{D,\mathrm{free}} = & -\frac{1}{2}\left(\Phi^{\mu\nu}_{D^*}\right)^\dagger \Phi_{D^*\,\mu\nu} - \frac{1}{2}\left(\Phi^{\mu\nu}_{D_s^*}\right)^\dagger \Phi_{D_s^*\,\mu\nu} \\
& + \left(D_\mu \Phi_D\right)^\dagger D^\mu \Phi_D + \left(D_\mu \Phi_{D_s}\right)^\dagger D^\mu \Phi_{D_s} \\
& + m_D^2 \left[\left(\Phi^\mu_{D^*}\right)^\dagger \Phi_{D^*\,\mu} + \left(\Phi^\mu_{D_s^*}\right)^\dagger \Phi_{D_s^*\,\mu}\right] \\
& - m_D^2 \left[\Phi_D^\dagger \Phi_D + \Phi_{D_s}^\dagger \Phi_{D_s}\right] + \mathrm{h.c.}\,.
\end{aligned}
$$

Model

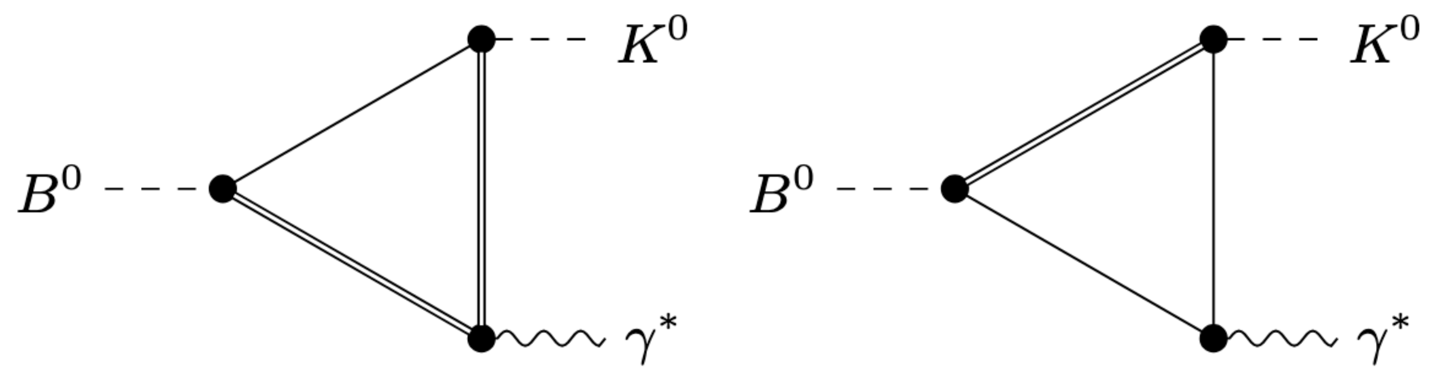

* **Dynamics of $D^{(*)}_{(s)}$ mesons close to their mass shell, determined by:**
  * Lorentz + Gauge invariance under QED
  * $SU(3)$ light-flavor symmetry
  * Heavy-quark spin symmetry

$$\mathcal{L}_{D,\text{free}} = -\frac{1}{2}\left(\Phi^{\mu\nu}_{D^*}\right)^\dagger \Phi_{D^*\,\mu\nu} - \frac{1}{2}\left(\Phi^{\mu\nu}_{D^*_s}\right)^\dagger \Phi_{D^*_s\,\mu\nu}$$
$$+ \left(D_\mu \Phi_D\right)^\dagger D^\mu \Phi_D + \left(D_\mu \Phi_{D_s}\right)^\dagger D^\mu \Phi_{D_s}$$
$$+ m_D^2 \left[\left(\Phi^\mu_{D^*}\right)^\dagger \Phi_{D^*\,\mu} + \left(\Phi^\mu_{D^*_s}\right)^\dagger \Phi_{D^*_s\,\mu}\right]$$
$$- m_D^2 \left[\Phi^\dagger_D \Phi_D + \Phi^\dagger_{D_s} \Phi_{D_s}\right] + \text{h.c.}\,.$$

* **Weak $B \to DD^*$ transition described by (using heavy-quark spin symmetry + data)**

$$\mathcal{L}_{BD} = g_{DD^*}\left(\Phi^{\mu\dagger}_{D^*_s}\,\Phi_D \partial_\mu \Phi_B + \Phi^\dagger_{D_s}\,\Phi^\mu_{D^*} \partial_\mu \Phi_B\right) + \text{h.c.}$$

In principle g_{DD^*} could have a phase -> we maximize over it

Model

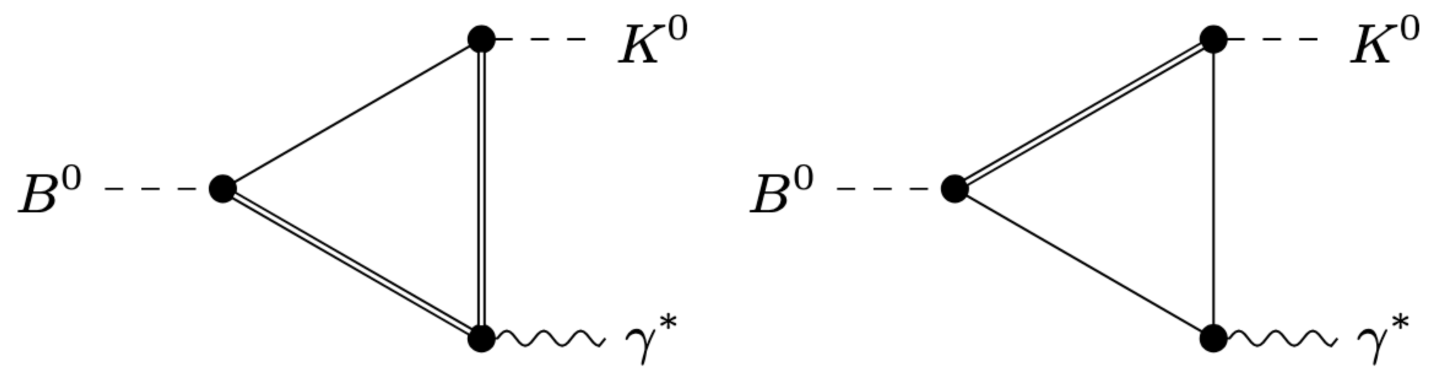

* **Dynamics of $D^{(*)}_{(s)}$ mesons close to their mass shell, determined by:**
  * Lorentz + Gauge invariance under QED
  * $SU(3)$ light-flavor symmetry
  * Heavy-quark spin symmetry

$$\mathcal{L}_{D,\text{free}} = -\frac{1}{2}\left(\Phi^{\mu\nu}_{D^*}\right)^\dagger \Phi_{D^*\,\mu\nu} - \frac{1}{2}\left(\Phi^{\mu\nu}_{D^*_s}\right)^\dagger \Phi_{D^*_s\,\mu\nu} + \left(D_\mu \Phi_D\right)^\dagger D^\mu \Phi_D + \left(D_\mu \Phi_{D_s}\right)^\dagger D^\mu \Phi_{D_s} + m_D^2\left[\left(\Phi^\mu_{D^*}\right)^\dagger \Phi_{D^*\,\mu} + \left(\Phi^\mu_{D^*_s}\right)^\dagger \Phi_{D^*_s\,\mu}\right] - m_D^2\left[\Phi^\dagger_D \Phi_D + \Phi^\dagger_{D_s}\Phi_{D_s}\right] + \text{h.c.}\,.$$

* **Weak $B \to DD^*$ transition described by (using heavy-quark spin symmetry + data)**

$$\mathcal{L}_{BD} = g_{DD^*}\left(\Phi^{\mu\dagger}_{D^*_s}\,\Phi_D \partial_\mu \Phi_B + \Phi^\dagger_{D_s}\,\Phi^\mu_{D^*}\partial_\mu \Phi_B\right) + \text{h.c.}$$

In principle g_{DD^*} could have a phase -> we maximize over it

* **From HHChPT** (valid close to endpoint $q^2 \approx m_B^2$):

$$\mathcal{L}_{DK} = \frac{2 i g_\pi m_D}{f_K}\left(\Phi^{\mu\dagger}_{D^*}\,\Phi_{D_s}\partial_\mu \Phi^\dagger_K - \Phi^\dagger_D \Phi^\mu_{D^*_s}\partial_\mu \Phi^\dagger_K\right) + \text{h.c.}$$

Model

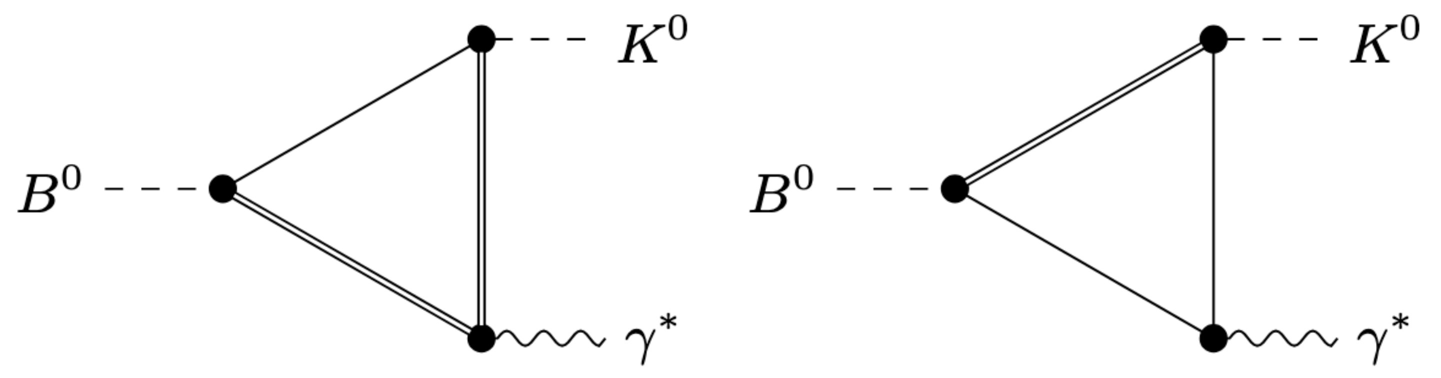

- **Dynamics of $D^{(*)}_{(s)}$ mesons close to their mass shell, determined by:**
  - Lorentz + Gauge invariance under QED
  - $SU(3)$ light-flavor symmetry
  - Heavy-quark spin symmetry

$$\mathcal{L}_{D,\text{free}} = -\frac{1}{2}\left(\Phi^{\mu\nu}_{D^*}\right)^\dagger \Phi_{D^*\,\mu\nu} - \frac{1}{2}\left(\Phi^{\mu\nu}_{D^*_s}\right)^\dagger \Phi_{D^*_s\,\mu\nu} + \left(D_\mu \Phi_D\right)^\dagger D^\mu \Phi_D + \left(D_\mu \Phi_{D_s}\right)^\dagger D^\mu \Phi_{D_s} + m_D^2\left[\left(\Phi^\mu_{D^*}\right)^\dagger \Phi_{D^*\,\mu} + \left(\Phi^\mu_{D^*_s}\right)^\dagger \Phi_{D^*_s\,\mu}\right] - m_D^2\left[\Phi^\dagger_D \Phi_D + \Phi^\dagger_{D_s}\Phi_{D_s}\right] + \text{h.c.}\,.$$

- **Weak $B \to DD^*$ transition described by (using heavy-quark spin symmetry + data)**

$$\mathcal{L}_{BD} = g_{DD^*}\left(\Phi^{\mu\dagger}_{D^*_s}\,\Phi_D \partial_\mu \Phi_B + \Phi^\dagger_{D_s}\,\Phi^\mu_{D^*}\partial_\mu \Phi_B\right) + \text{h.c.}$$

In principle g_{DD^*} could have a phase -> we maximize over it

- **From HHChPT** (valid close to endpoint $q^2 \approx m_B^2$):

$$\mathcal{L}_{DK} = \frac{2ig_\pi m_D}{f_K}\left(\Phi^{\mu\dagger}_{D^*}\,\Phi_{D_s}\partial_\mu \Phi^\dagger_K - \Phi^\dagger_D \Phi^\mu_{D^*_s}\partial_\mu \Phi^\dagger_K\right) + \text{h.c.}$$

In the $SU(3)$-symmetric limit, the diagrams obtained by swapping $D_s^{(*)} \leftrightarrow D^{(*)}$ are symmetric.

Form factors

* To obtain a reliable estimate **over the entire kinematical range,** we introduce the form factors:

- **Correction for QED vertex**

$$e \to eF_V(q^2)\,, \quad F_V(q^2) = \begin{cases} 1\,, & q^2 = 0\,, \\ \sim q^{-2}\,, & q^2 \gg m_D^2 \end{cases}$$

  - Vector meson dominance Ansatz:

$$F_V(q^2) = \frac{m_{J/\psi}^2}{m_{J/\psi}^2 - q^2}$$

the change of sign from the low- to the high-q^2 region is a general feature

- **Correction for DD^*K vertex**

  - The model produces a $K-$emission amplitude that grows as E_K/f_K (correct only for soft-kaon limit)

$$\frac{1}{f_K} \to \frac{1}{f_K} G_K(q^2)\,,$$

$$G_K(q^2) = \frac{1}{1 + E_K(q^2)/f_K} = \frac{2m_B f_K}{2m_B f_K + m_B^2 - q^2}$$

Results

- Sum of diagrams shows an **ultraviolet divergence**; we use an $\overline{MS}$-like renormalization scheme to discard it and use the scale dependence to estimate the uncertainty.
- **Result** for these long-distance contributions in the $SU(3)-$ and heavy-quark spin symmetric limit:

$$\mathcal{M}_{\rm LD} = -\frac{e g_{DD^*} g_\pi F_V(q^2) G_K(q^2)}{8\pi^2 f_K m_D}(p_B \cdot j_{\rm em}) \times \left[\left(2+L_\mu\right) - \delta L(q^2, m_B^2, m_D^2)\right],$$

$$L_\mu = \log\left(\mu^2/m_D^2\right)$$

$$\delta L(q^2, m_B^2, m_D^2) = \frac{L(m_B^2, m_D^2) - L(q^2, m_D^2)}{q^2 - m_B^2},$$

$$L(x,y) = \log\left(\frac{2y - x + \sqrt{x(x-4y)}}{2y}\right) \times \left[\sqrt{x(x-4y)} + y \log\left(\frac{2y - x + \sqrt{x(x-4y)}}{2y}\right)\right]$$

- Compare it to the **short-distance matrix element:**

$$\mathcal{M}_{\rm SD} = \frac{4G_F}{\sqrt{2}} \frac{e}{16\pi^2} V_{tb}^* V_{ts} (p_B \cdot j_{\rm em}) f_+(q^2)(2C_9)$$

Results

- LD contributions do not exceed a few percent relative to the SD one.
- The **absorptive part** is independent of the renormalization scheme used, and corresponds to the analytic discontinuity of the amplitude corresponding to the kinematical regions where the internal mesons go on-shell.
- It can be considered model-independent at least at high q^2.
- We have separately checked the discontinuities, finding agreement with the loop calculation.

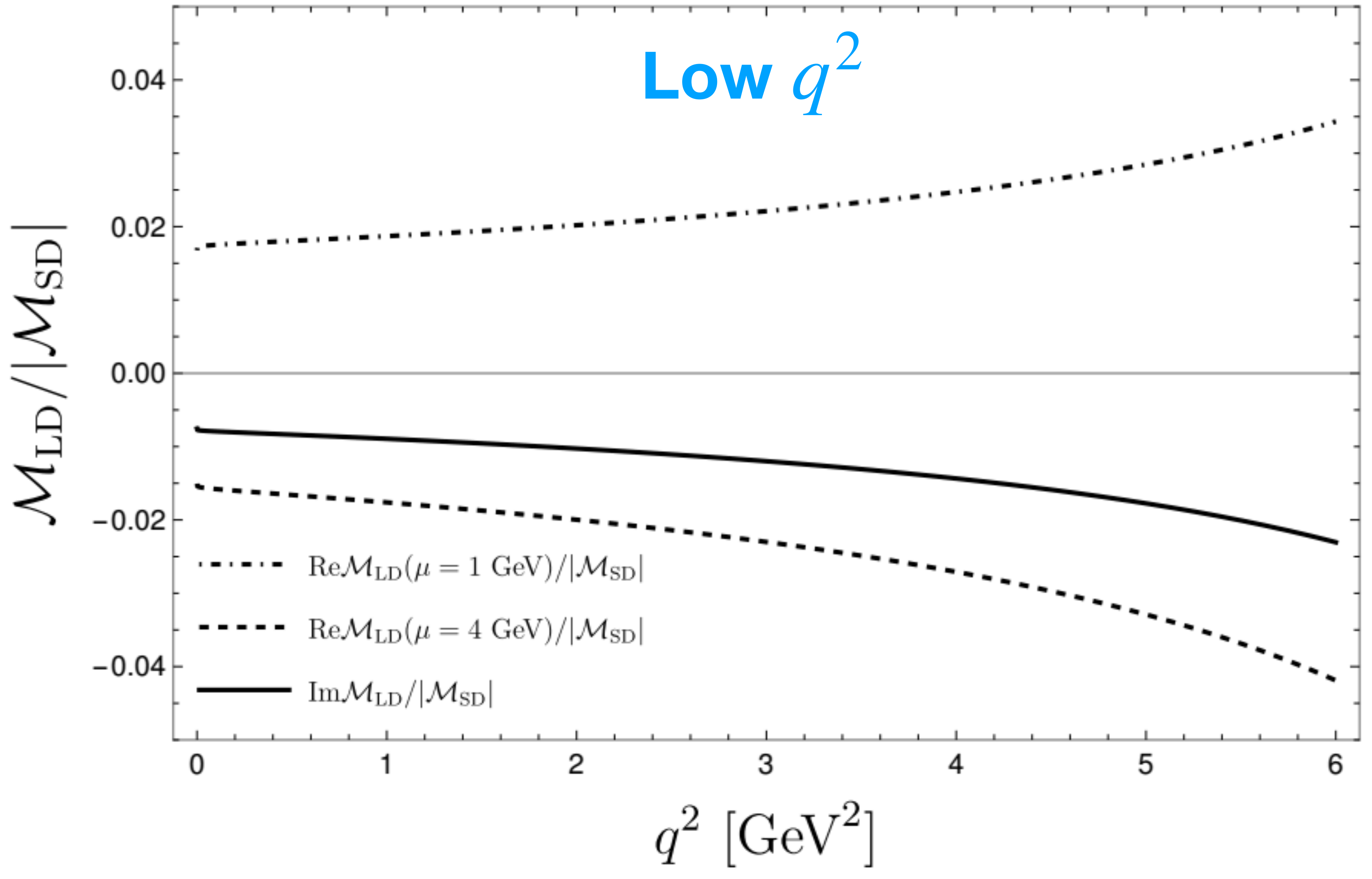

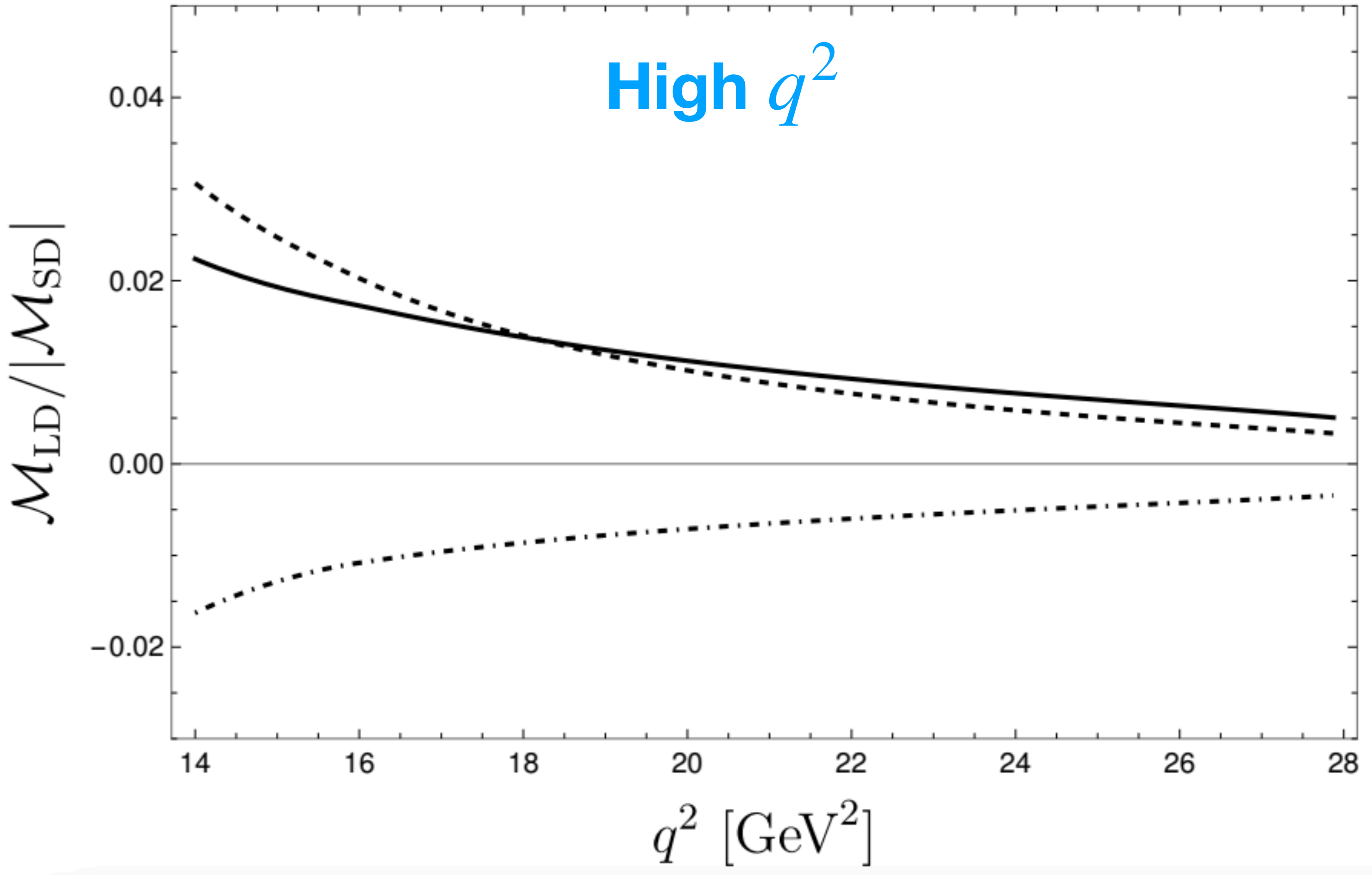

Effective shift in C_9

- We can encode the effect of the $\mathscr{M}_{LD}$ via a q^2-**dependent shift in** C_9**:**

$$\delta C^{\mathrm{LD}}_{9,DD^*}(q^2,\mu) = \bar{g}\,\Delta(q^2)\Big[2 + L_\mu - \delta L(q^2, m_B^2, m_D^2)\Big] \qquad \Delta(q^2) = -\frac{g_\pi m_B F_V(q^2) G_K(q^2)}{2 f_K f_+(q^2)}$$

- Averaging over the low- and high-q^2 regions, we find:

$$\delta\bar{C}^{\mathrm{LD,low}}_{9,DD^*}(\mu) = -0.003 - 0.059\,i - 0.156\log\left(\frac{\mu}{m_D}\right)$$

$$\delta\bar{C}^{\mathrm{LD,high}}_{9,DD^*}(\mu) = 0.009 + 0.053\,i + 0.063\log\left(\frac{\mu}{m_D}\right).$$

- Varying the renormalization scale μ in the range $[1,4]$ GeV:

$$|\delta\bar{C}^{\mathrm{LD}}_{9,DD^*}| \leq 0.11 \qquad \boxed{\frac{\delta C_9}{C_9^{SM}} \approx 2.5\,\%}$$

Accounting for additional intermediate states

- So far we focused on the D^*D_s or D_s^*D intermediate states, but in principle there are **other states** with $\bar{c}c\bar{s}d$ valence structure.
- Consider all intermediate states the allow parity-conserving strong interactions with the kaon.

- Conservative **multiplicity factor** accounting for all possible intermediate states:

$$\mathcal{N} = \frac{\sum_X \mathcal{M}(B^0 \to X)}{\mathcal{M}(B^0 \to D^* D_s) + \mathcal{M}(B^0 \to D D_s^*)} \approx \frac{1}{2} \sum_X \sqrt{\frac{\mathcal{B}(B^0 \to X)}{\mathcal{B}(B^0 \to D D_s^*)}} \approx 3$$

$$|\delta C_9^{\rm LD}| \leq \mathcal{N} |\delta \bar{C}_{9,DD^*}^{\rm LD}| \leq 0.33 \quad \longrightarrow \quad \frac{\delta C_9}{C_9^{SM}} \approx 8 - 10\,\%$$

B^0 Decay	$\mathcal{B}(B^0 \to X) \times 10^3$
$D^* D_s$	8.0 ± 1.1
$D D_s^*$	7.4 ± 1.6
$D^* D_s^*$	17.7 ± 1.4
$D D_{s0}(2317)$	1.06 ± 1.6
$D^* D_{s1}(2457)$	9.3 ± 2.2
$D^* D_{s1}(2536)$	0.50 ± 0.14
$D D_{s2}(2573)$	$(3.4 \pm 1.8) \times 10^{-2}$
$D^* D_{s2}(2573)$	< 0.2
$D D_{s1}(2700)$	0.71 ± 0.12

Sign of δC_9

- The sign of δC_9 is **opposite** in the two cases (regardless of the phase of g_{DD*}): comparing the extraction of C_9 at low- and high-q^2 provides a useful data-driven check for such long-distance contributions.

Sign of δC_9

- The sign of δC_9 is **opposite** in the two cases (regardless of the phase of g_{DD^*}): comparing the extraction of C_9 at low- and high-q^2 provides a useful data-driven check for such long-distance contributions.

2014 LHCb,
2023 CMS

2016 and
2020 LHCb

- We perform a fit of C_9 from the branching ratio and angular observables in $B \to K^* \bar{\mu}\mu$, assuming:

$$C_9 \to C_9^\lambda(q^2) + Y_{q\bar{q}}^{[0]}(q^2) + Y_{b\bar{b}}^{[0]}(q^2) + Y_{c\bar{c}}^\lambda(q^2)$$

encodes (factorizable) perturbative contributions from 4-quark operators

encodes the perturbative charm-loop contributions and $c\bar{c}$ resonances

$$Y_{c\bar{c}}^\lambda(q^2) = Y_{c\bar{c}}^\lambda(q_0^2) + \frac{16\pi^2}{\mathcal{F}_\lambda(q^2)} \Delta\mathcal{H}_{c\bar{c}}^\lambda(q^2), \; q_0^2 = 0$$

$$\Delta\mathcal{H}_{c\bar{c}}^{\lambda,1P} = \sum_V \eta_V^\lambda e^{i\delta_V^\lambda} \frac{q^2}{m_V^2} A_V^{\text{res}}(q^2) \qquad A_V^{\text{res}}(q^2) = \frac{m_V \Gamma_V}{m_V^2 - q^2 - i m_V \Gamma_V}$$

- We extract the residual contribution to C_9 from data:

$$C_9^\lambda(q^2) = C_9^{\text{SM}} + C_9^{\text{LD},\lambda}(q^2) + C_9^{\text{SD}}$$

Short-distance, independent of λ and q^2

Long-distance, no reason to assume it is independent of λ or q^2

[M. Bordone, G.Isidori, S. Mächler, AT, 2401.18007]

Sign of δC_9

Using resonance parameters found by LHCb recently (2405.17347)

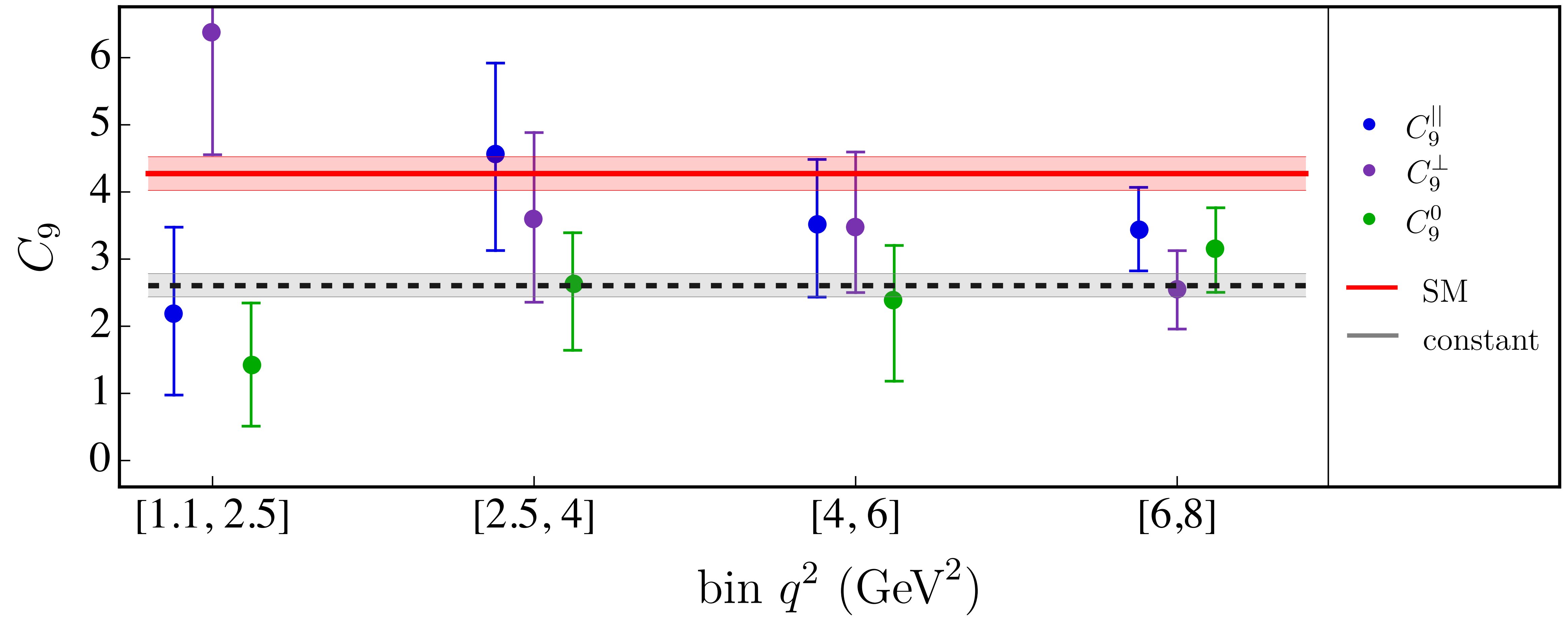

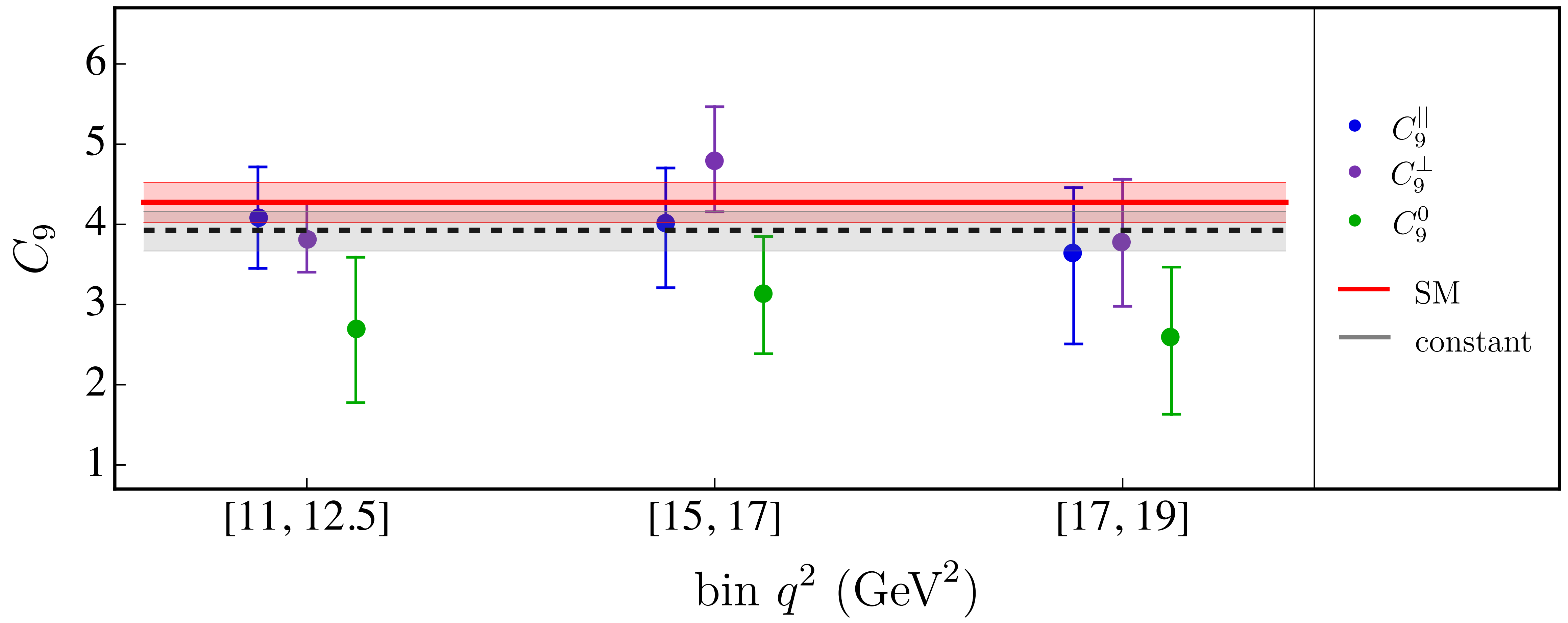

	constant C_9	$C_9^{\|\|}$	$C_9^{\perp}$	C_9^{0}
Low q^2	$2.60^{+0.18}_{-0.17}$	$2.4^{+0.6}_{-0.6}$	$2.6^{+0.7}_{-0.6}$	$2.8^{+0.7}_{-0.8}$
High q^2	$3.93^{+0.23}_{-0.26}$	$4.0^{+0.5}_{-0.5}$	$4.0^{+0.4}_{-0.4}$	$2.9^{+0.6}_{-0.6}$

$$C_9 = 3.40^{+0.16}_{-0.16} \quad (\chi^2/dof = 1.5)$$

The shift in C_9 we find from charm rescattering + NP shift of ~-1 gives a better global fit than a shift of ~-1

Importance of extracting the value of C_9 at different values of q^2

Conclusions

* Non-local contributions in $b \to s\bar{\ell}\ell$ could significantly impact the extraction of C_9.
* We have presented an estimate of $B^0 \to K^0\bar{\ell}\ell$ long-distance contributions induced by the rescattering of a charmed and a charmed-strange meson;
* At **high** q^2 the estimate is based on controlled approximations from VMD and HHChPT; at **low** q^2 the extrapolation via form factors is only meant to provide a conservative upper bound;
* For the particular intermediate state we considered, charm rescattering contributions don't seem to be very large. We neglected some effects, but we conservatively accounted for additional intermediate states.

Conclusions

- Non-local contributions in $b \to s\bar{\ell}\ell$ could significantly impact the extraction of C_9.
- We have presented an estimate of $B^0 \to K^0\bar{\ell}\ell$ long-distance contributions induced by the rescattering of a charmed and a charmed-strange meson;
- At **high** q^2 the estimate is based on controlled approximations from VMD and HHChPT; at **low** q^2 the extrapolation via form factors is only meant to provide a conservative upper bound;
- For the particular intermediate state we considered, charm rescattering contributions don't seem to be very large. We neglected some effects, but we conservatively accounted for additional intermediate states.
- Going forward:
  - At the experimental level, the extraction of C_9 at different values of q^2 is key.
  - At the theoretical level, extension of this method: inclusion of the dipole coupling for the $DD^*\gamma$ vertex, more complicated intermediate states, different modes ($B \to K^*$)…

Thank you for your attention!

Backup Slides

Rules

$KDD*$

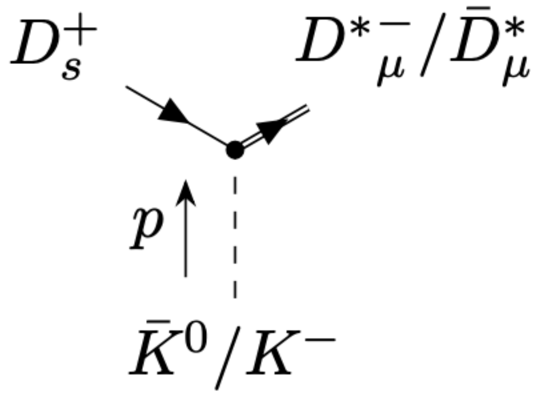

$$= \frac{2ig_\pi m_{D^*D_s}}{f} p_\mu \quad ,$$

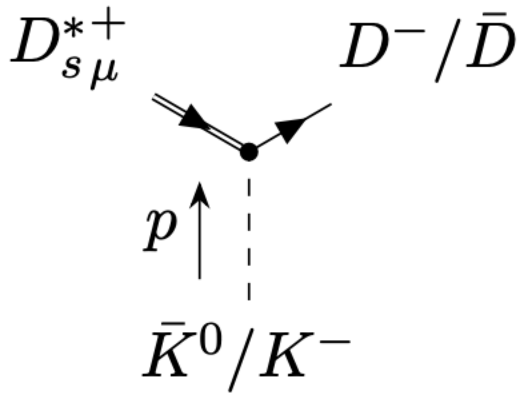

$$= -\frac{2ig_\pi m_{DD_s^*}}{f} p_\mu$$

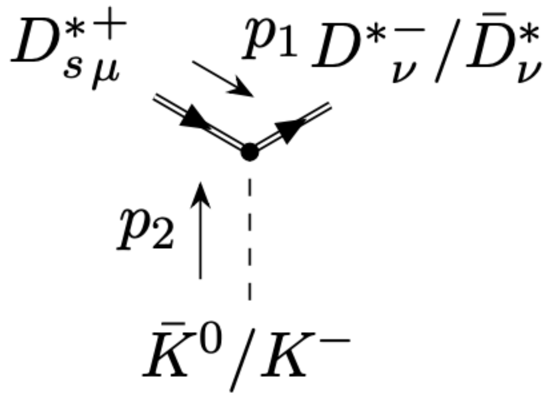

$$= -\frac{2ig_\pi}{f}\sqrt{\frac{m_{D^*}}{m_{D_s^*}}} p_1^\alpha p_2^\beta \epsilon_{\alpha\beta\mu\nu}$$

$BDD*$

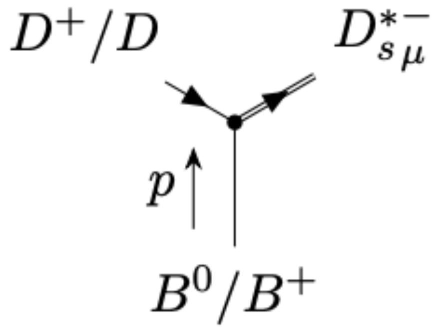

$$= e^{i\varphi_*} g_{DD^*} p_\mu \quad ,$$

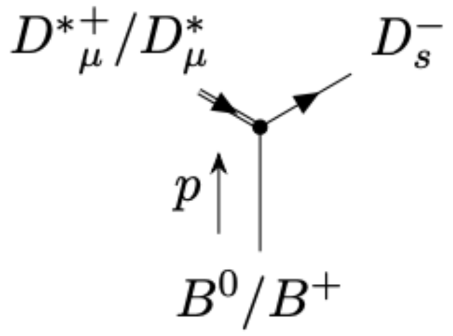

$$= e^{-i\varphi_*} g_{DD^*} p_\mu$$

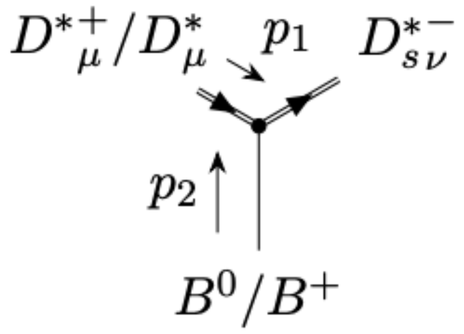

$$= -\, e^{i\varphi_{**}} g_{D^*D^*} p_1^\alpha p_2^\beta \epsilon_{\alpha\beta\mu\nu}$$

$DD\gamma$ and $DD\gamma K$

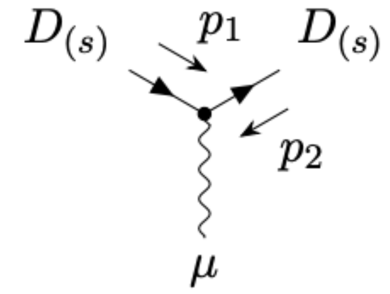

$$= ieQ_D(p_{1\mu} - p_{2\mu})$$

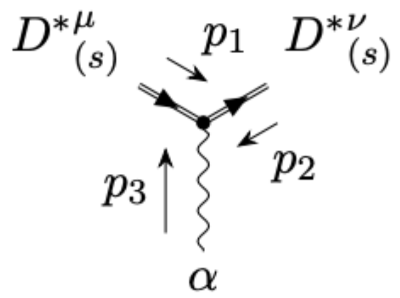

$$= ieQ_{D^*}\left[p_{2\nu}\eta_{\mu\alpha} - p_{1\mu}\eta_{\nu\alpha} + (p_{1\alpha} - p_{2\alpha})\eta_{\mu\nu}\right]$$

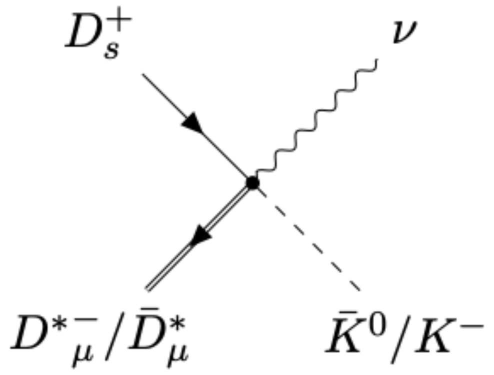

$$= \frac{2ig_\pi\sqrt{m_D m_{D^*}}}{f}\, e\, Q_K\, \eta_{\mu\nu}$$

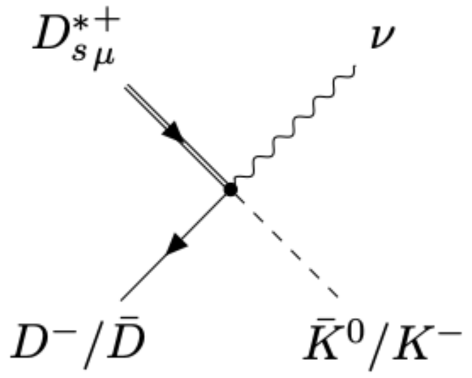

$$= -\frac{2ig_\pi\sqrt{m_D m_{D^*}}}{f}\, e\, Q_K\, \eta_{\mu\nu}$$

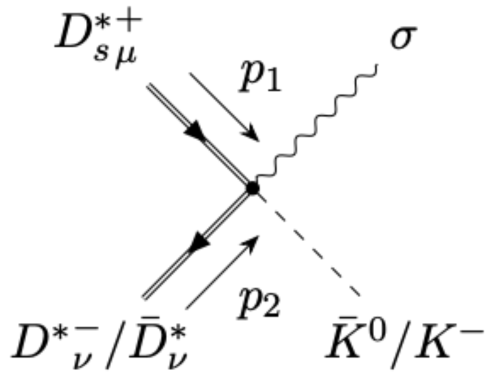

$$= \frac{2ig_\pi}{f}\sqrt{\frac{m_{D^*}}{m_{D_s^*}}}\, e\,({p_2}^\alpha + {p_1}^\alpha Q_{D^*})\, \epsilon_{\alpha\mu\nu\sigma}$$

Diagrams

Neutral case

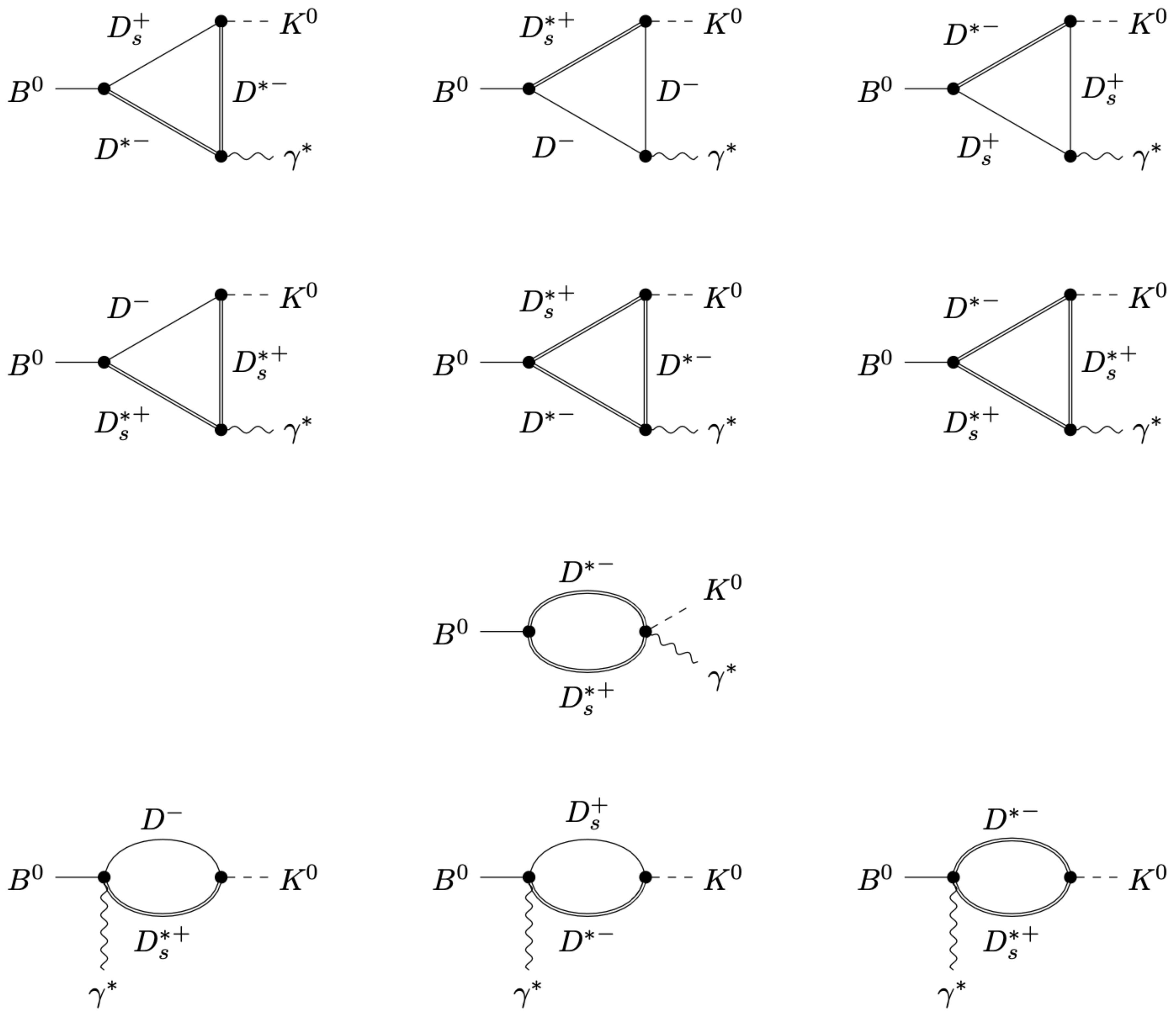

Charged case

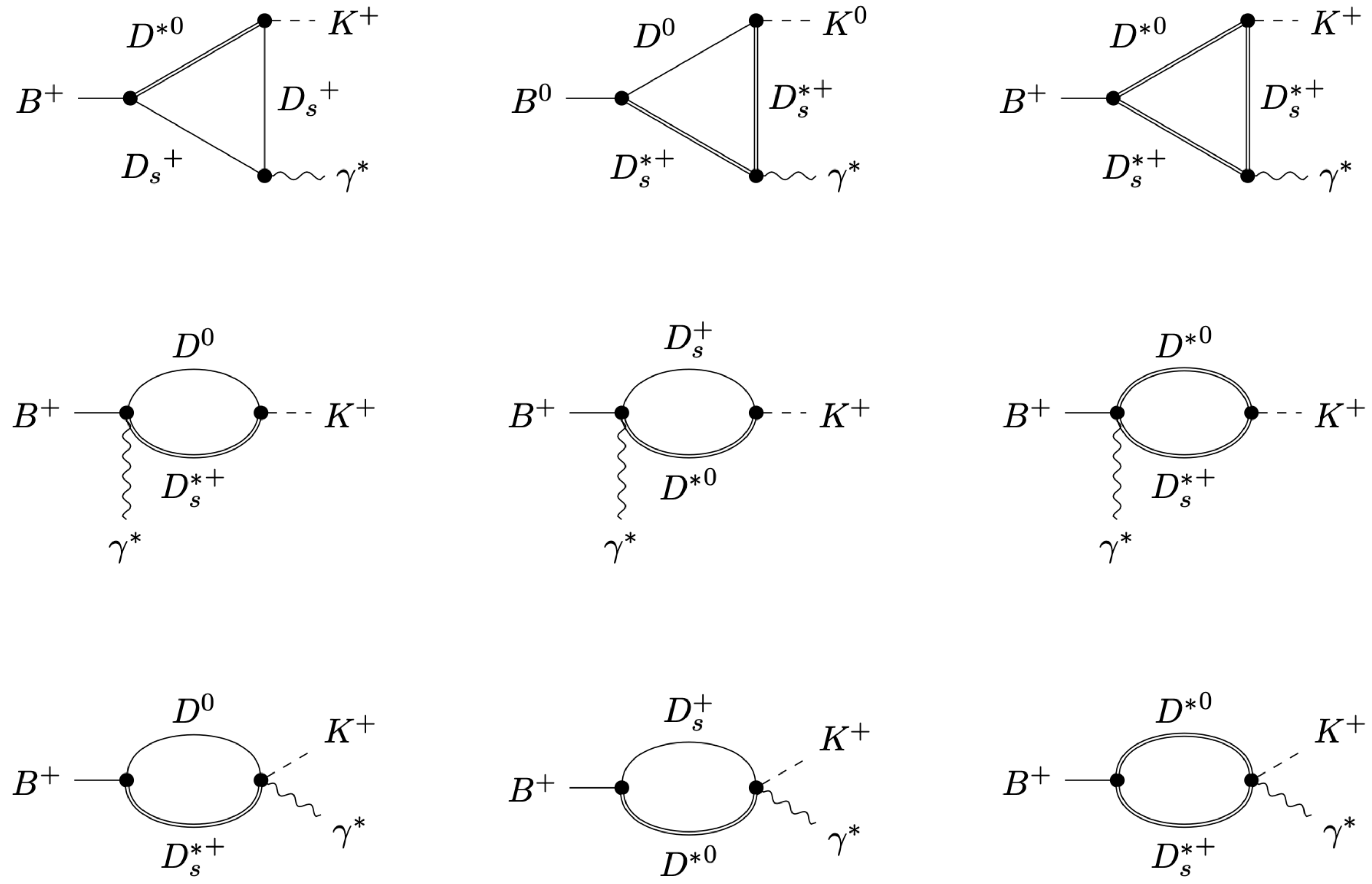

Fit

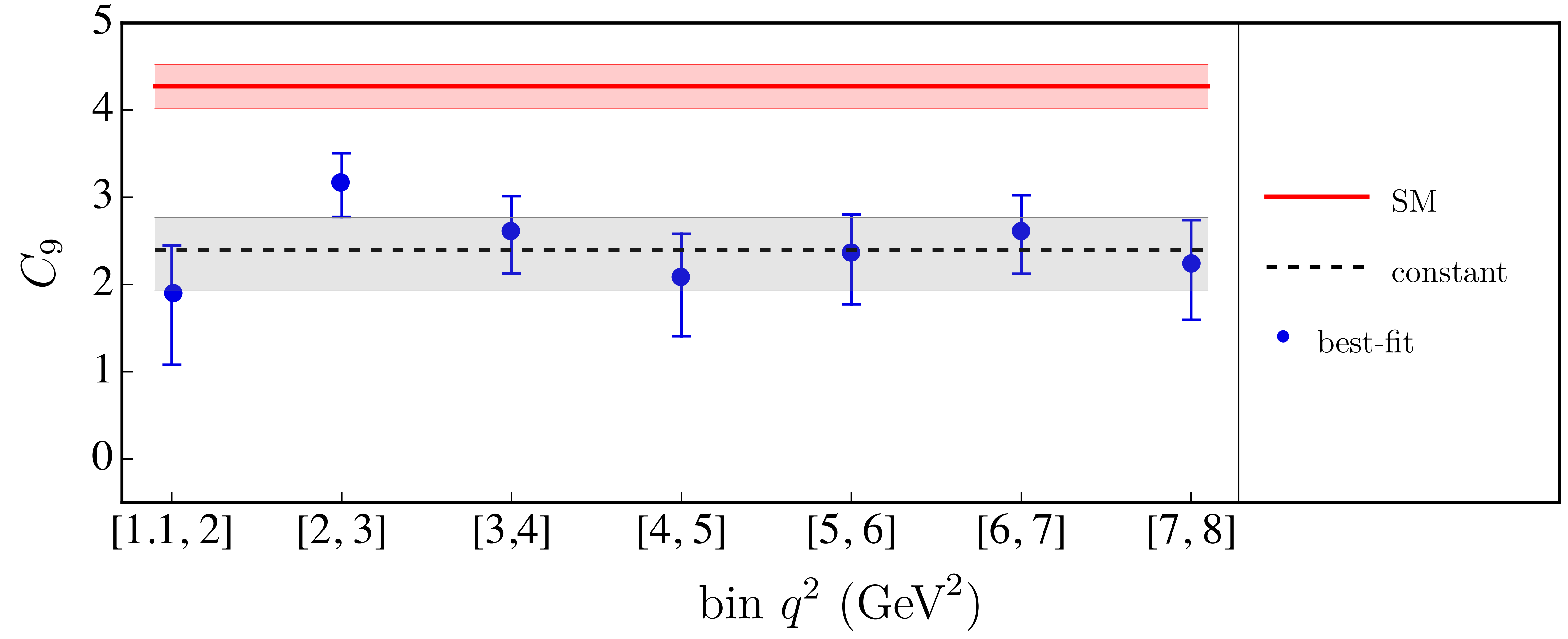

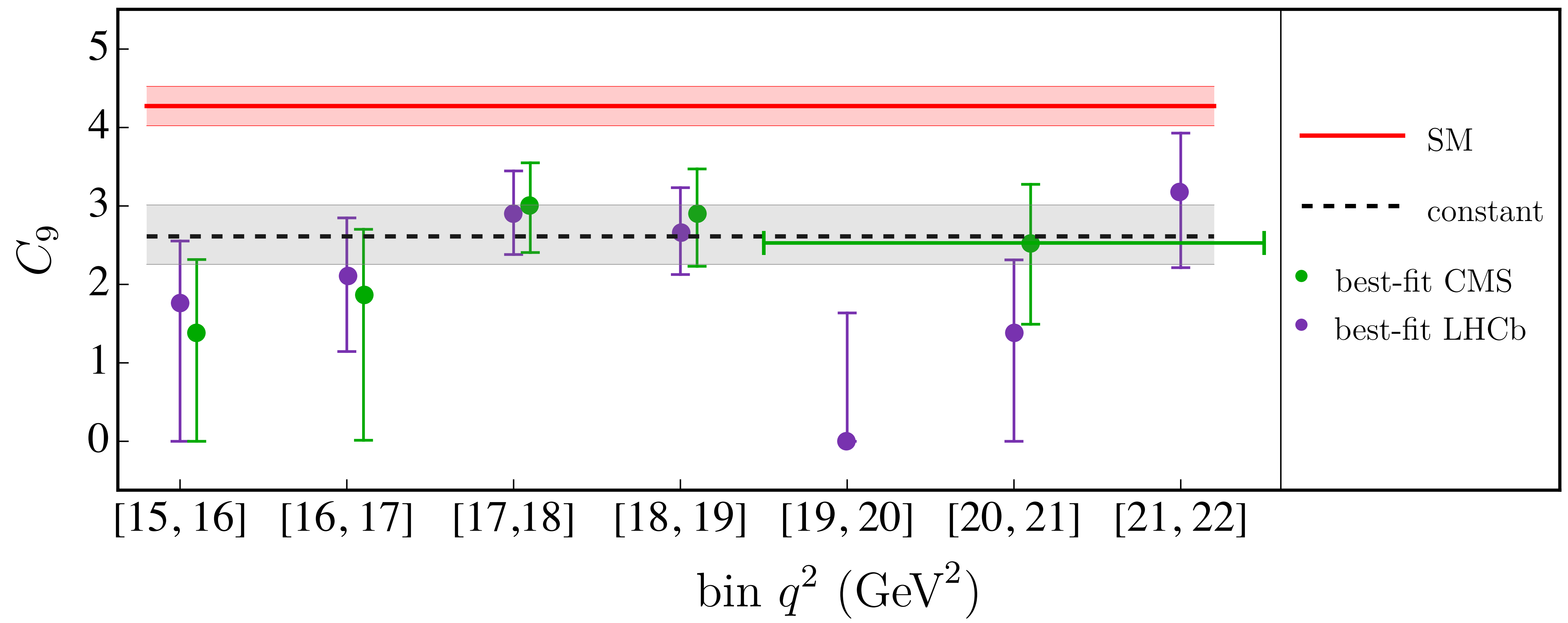

q^2 (GeV^2)	C_9^K
[1.1, 2]	$1.9^{+0.5}_{-0.8}$
[2, 3]	$3.2^{+0.3}_{-0.4}$
[3, 4]	$2.6^{+0.4}_{-0.5}$
[4, 5]	$2.1^{+0.5}_{-0.7}$
[5, 6]	$2.4^{+0.4}_{-0.6}$
[6, 7]	$2.6^{+0.4}_{-0.5}$
[7, 8]	$2.3^{+0.5}_{-0.7}$
constant	$2.4^{+0.4}_{-0.5}$ ($\chi^2/\mathrm{dof} = 1.35$)

q^2 (GeV^2)	C_9^K (LHCb)	C_9^K (CMS)
[15, 16]	$1.8^{+0.8}_{-1.8}$	$1.4^{+0.9}_{-1.4}$
[16, 17]	$2.1^{+0.7}_{-1.0}$	$1.9^{+0.8}_{-1.9}$
[17, 18]	$2.9^{+0.5}_{-0.5}$	$3.0^{+0.5}_{-0.6}$
[18, 19]	$2.7^{+0.6}_{-0.5}$	
[18, 19.24]		$2.9^{+0.6}_{-0.7}$
[19, 20]	$0^{+1.6}_{-0}$	
[20, 21]	$1.4^{+0.9}_{-1.4}$	
[21, 22]	$3.2^{+0.8}_{-0.9}$	
[19.24, 22.9]		$2.5^{+0.7}_{-1.0}$
constant	2.6 ± 0.4 ($\chi^2/\mathrm{dof} = 1.06$)	

Table 3.3: Determinations of C_9 from $B \to K\mu^+\mu^-$ in the low-q^2 (left) and high-q^2 (right) regions. The p-values for the constant fits are 0.17 (low-q^2) and 0.39 (high-q^2).

[M. Bordone, G.Isidori, S. Mächler, AT, 2401.18007]

Form factors

* Correction for DD^*K **vertex**:

$$\frac{1}{f_K} \to \frac{1}{f_K} G_K(q^2)\,,$$
$$G_K(q^2) = \frac{1}{1 + E_K(q^2)/f_K} = \frac{2m_B f_K}{2m_B f_K + m_B^2 - q^2}$$

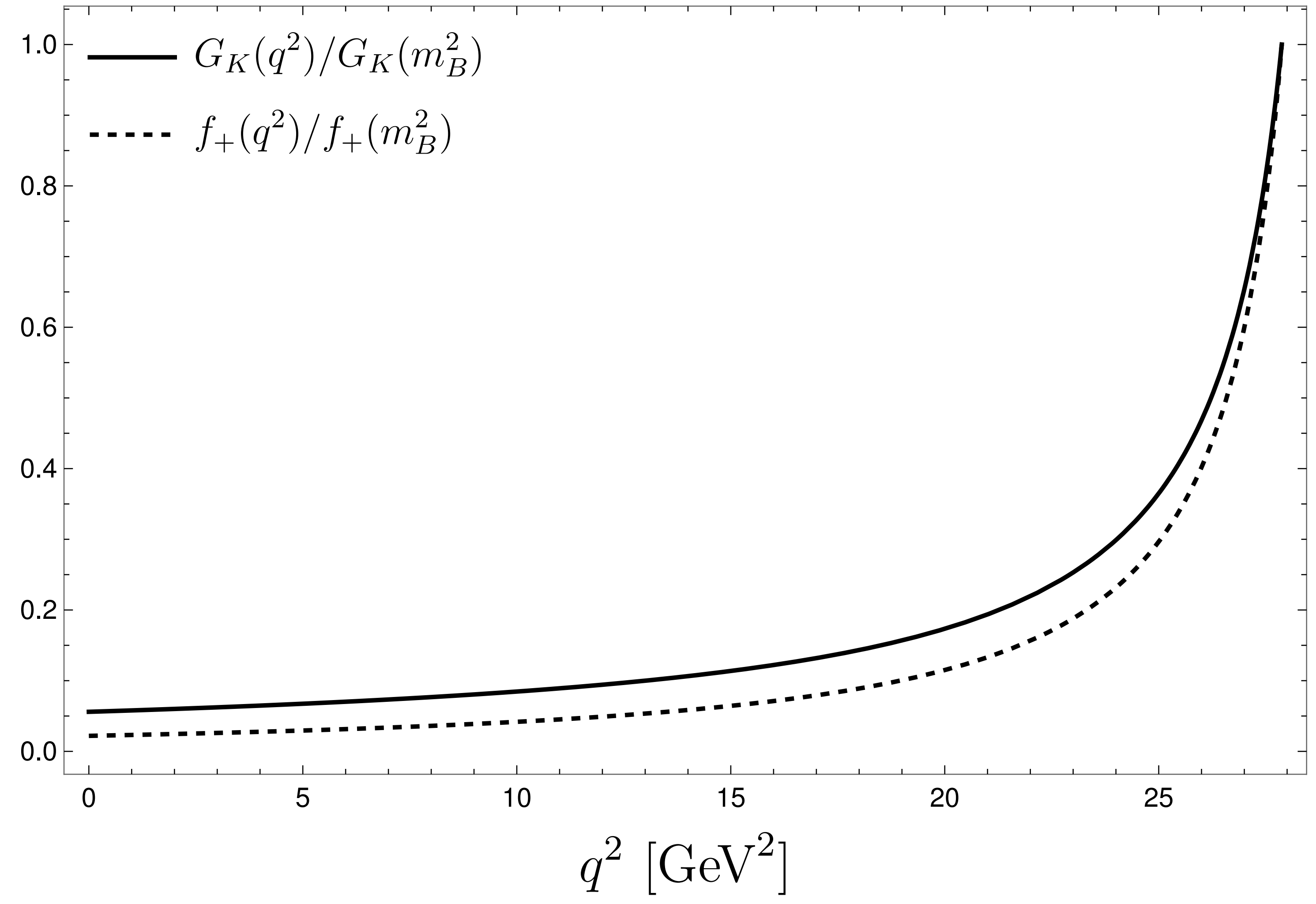

Useful consistency check: G_K has a similar scaling to the vector form factor $f_+(q^2)$ for $B_0 \to K_0$